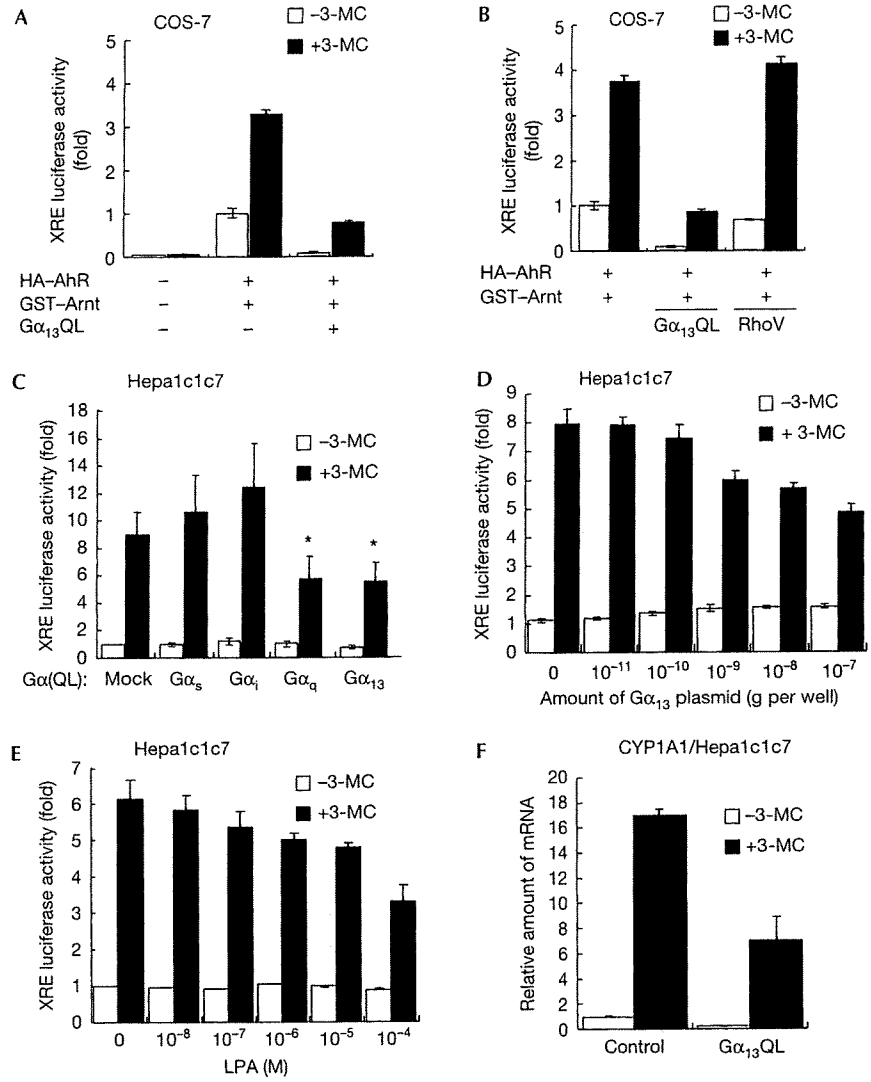

Fig 2 | Activated $G\alpha_{13}$ inhibits AhR-mediated transcriptional activity. (**A**,**B**) COS-7 cells transfected as indicated were stimulated with 1 μM 3-MC and then used for the luciferase reporter gene analysis. (**C**,**D**) Hepa1c1c7 cells expressing constitutively active mutants of Gα were stimulated with or without 1 μM 3-MC for 24 h, and then the luciferase reporter gene analysis was performed. In (**D**), Hepa1c1c7 cells were transfected with various amounts of $G\alpha_{13}$Q226L. (**E**) Hepa1c1c7 cells harbouring a reporter gene were pretreated with various concentrations of LPA, and were then stimulated with 3-MC and used for reporter gene analysis. (**F**) Hepa1c1c7 cells transfected with or without $G\alpha_{13}$Q226L were treated with 1 μM 3-MC for 12 h. The expression of CYP1A1 was analysed by the quantitative RT–PCR method. Error bar means s.e. ($n = 3$, $^*P < 0.05$). 3-MC, 3-methyl cholanthrene; AhR, aryl hydrocarbon receptor; GST, glutathione *S*-transferase; HA, haemagglutinin; LPA, lysophosphatidic acid; RT–PCR, reverse transcription–PCR.

(Fig 2B). These data suggest that the active $G\alpha_{13}$ inhibits the activation of AhR in a RhoA-independent manner. Next, we tested the effect of various Gα-subunits on endogenous activation of AhR using Hepa1c1c7 cells, which express highly the endogenous AhR and AIP. As shown in Fig 2C, $G\alpha_{13}$Q226L and $G\alpha_q$Q209L inhibited the XRE-driven luciferase activity and $G\alpha_{13}$Q226L showed the dose-dependent inhibition of AhR (Fig 2D). The Gα specificity of suppression of luciferase activity was correlated with the ability of Gα to bind to AIP (Figs 1C,2C), implying that the interaction of Gα with AIP could trigger the suppression of AhR. LPA is known to activate $G\alpha_{13}$ through its receptor. Stimulation by LPA also suppressed 3-MC-induced activation of AhR in a dose-dependent manner (Fig 2E), indicating that the physiological activation of the $G\alpha_{13}$ signal suppresses the activation of AhR. Next, we investigated the effect of $G\alpha_{13}$ on AhR-induced CYP1A1 expression using quantitative reverse transcription–PCR (RT–PCR) analysis. In Hepa1c1c7 cells, 3-MC induced the expression of CYP1A1, and this induction was markedly decreased when $G\alpha_{13}$Q226L was expressed (Fig 2F). These data suggest that the activation of $G\alpha_{13}$ inhibits the AhR-mediated transcriptional activity.

The localization of AhR is altered by $G\alpha_{13}$

AhR is a nucleocytoplasmic shuttling protein, and AIP is crucial in the cytoplasmic localization of AhR (Petrulis *et al*, 2003). To examine the effect of $G\alpha_{13}$ on the localization of AhR, we

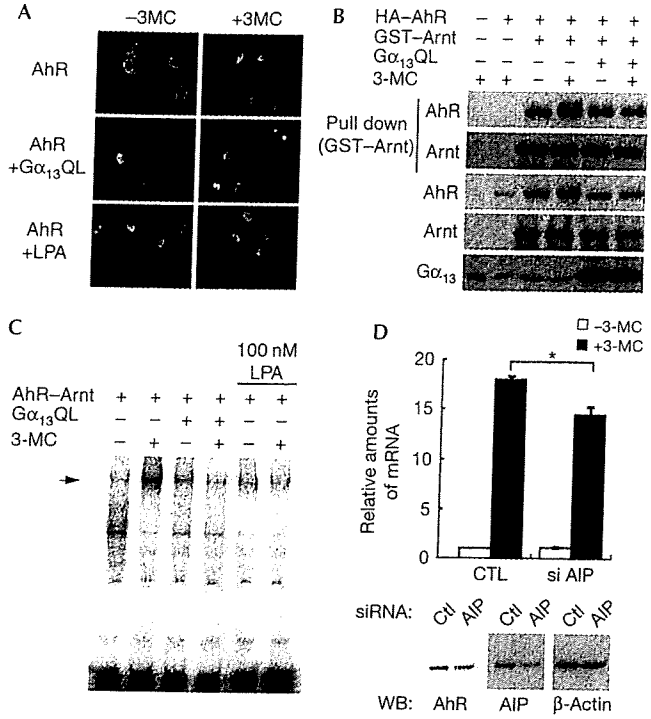

Fig 3 | The subcellular localization, dimerization with Arnt and DNA-binding activity of AhR are altered by the activation of $G\alpha_{13}$. (A) COS-7 cells expressing HA–AhR, GST–Arnt or $G\alpha_{13}Q226L$ were stimulated with 3-MC and/or LPA for 24 h. The localization of AhR was visualized by immunostaining with the HA antibody. (B) COS-7 cells transfected as indicated were stimulated with 1 μM 3-MC for 6 h. The protein complexes were precipitated and analysed by immunoblot analysis. (C) COS-7 cells transfected with the indicated combinations of plasmids were stimulated with 1 μM 3-MC for 6 h. Nuclear extracts were analysed by EMSA with the radioactively labelled AhR-binding element DNA probe. An arrow indicates the AhR–Arnt complex binding to the probe. (D) Hepa1c1c7 cells were transfected with the indicated siRNA mixture, and stimulated with 1 μM 3-MC for 12 h. The expression of CYP1A1 was analysed by the quantitative RT-PCR method. Expression of AhR, AIP and β-actin were analysed by immunoblot. 3-MC, 3-methyl cholanthrene; AhR, aryl hydrocarbon receptor; AIP, AhR-interacting protein; Ctl, control; EMSA, electrophoretic mobility shift assay; GST, glutathione *S*-transferase; HA, haemagglutinin; LPA, lysophosphatidic acid; RT–PCR, reverse transcription–PCR; siRNA, short interfering RNA.

examined by using immunofluorescence analysis where AhR localizes under the activation of $G\alpha_{13}$. Haemagglutinin-tagged AhR expressed in COS-7 cells was observed in the cytoplasm in quiescent cells. Once cells were stimulated by 3-MC, AhR translocated to the nucleus (Fig 3A). Interestingly, the expression of $G\alpha_{13}Q226L$ and LPA stimulation resulted in the nuclear translocation of AhR despite the absence of 3-MC (Fig 3A). It is known that an interaction between AhR and AIP is required for the localization of AhR in the cytoplasm, as well as for the ligand-mediated transcriptional activation of AhR (Meyer *et al*, 1998). As $G\alpha_{13}$ inhibited the association of AhR with AIP (Fig 1E), the $G\alpha_{13}$-induced dissociation of AhR from AIP might lead to the translocation of AhR to the nucleus. Although 3-MC induced the translocation of AhR to the nucleus followed by the transactivation of AhR, the nuclear localization of AhR induced by $G\alpha_{13}$ failed to induce the transactivation of AhR (Fig 2). To investigate whether nuclear-accumulated AhR by $G\alpha_{13}$ is not in an 'active state', we examined the effect of $G\alpha_{13}$ on the ability of AhR to interact with Arnt. We introduced GST–Arnt and AhR with or without $G\alpha_{13}Q226L$ into COS-7 cells, and then GST pull-down analysis was performed to detect the AhR/GST–Arnt protein complex. As shown in Fig 3B, the stimulation with 3-MC enhanced the complex formation of Arnt and AhR (Fig 3B, lanes 3 and 4). Interestingly, the expression of $G\alpha_{13}Q226L$ prevented the 3-MC-induced complex formation of Arnt and AhR (Fig 3B, lanes 5 and 6). This result suggests that AhR accumulated in the nucleus by $G\alpha_{13}$ is not in an active complex. To verify this hypothesis, we next tested by using an electrophoretic mobility shift assay (EMSA) whether the $G\alpha_{13}$ signal affects the binding activity of AhR to XRE. When AhR and Arnt were ectopically expressed in COS-7 cells, the nuclear extract from the cells treated with 3-MC showed binding activity to a DNA probe including XRE (supplementary Fig 1 online). The expression of $G\alpha_{13}Q226L$ prevented the 3-MC-induced DNA-binding activity of AhR (Fig 3C). LPA also inhibited the formation of the AhR–DNA complex. It is well established that the transcriptional activation of AhR requires a ligand-induced conformational change that confers the ability of nuclear translocation and heterodimer formation of AhR with Arnt. This heterodimer formation leads to their binding to an XRE element. By contrast, our results indicated that $G\alpha_{13}$ induces the nuclear accumulation of AhR without ligand stimulation. However, in the presence of the $G\alpha_{13}$ signal, AhR showed no ability to form the complex with Arnt and failed to bind to XRE, because of lacking the conformational change of AhR. Next, to test whether sequestering AIP from the AhR complex is enough for the $G\alpha_{13}$-induced suppressive effect on the activation of AhR, we used RNA interference to knock down AIP. The activation of AhR was partly reduced by small interfering RNA (siRNA) of AIP but could still be activated by 3-MC stimulation (Fig 3D). In addition, we fractionated the cytoplasm and nucleus from Hepa1c1c7 cells and analysed the localization of AhR. As shown in supplementary Fig 2 online, knockdown of AIP showed a fairly weak effect on AhR localization in the nucleus without 3-MC. The knockdown of AIP did not fully mimic the effect of $G\alpha_{13}$ on the AhR signal, indicating that $G\alpha_{13}$ not only disturbed the association between AhR and AIP but also affected other signals to suppress the activation of AhR. Lees & Whitelaw (2002) reported that antisense oligonucleotide for AIP decreased the activation of AhR in HEK293T cells. Conversely, it has also been reported that knockdown of AIP failed to shut down ligand-induced activation of AhR (Pollenz & Dougherty, 2005). Our current result seems to fall somewhere inbetween these two reports, and we have no additional information to explain this discrepancy. However, a study using an animal experiment showed that AIP is essential for AhR signalling (Lin *et al*, 2008). Clarification of the physiological role of AIP is a problem that needs to be explored.

$G\alpha_{13}$ promotes the destabilization of AhR

As described in the Introduction, in quiescent cells, AIP forms a stable complex with AhR and protects it from degradation by the ubiquitin–proteasome pathway. We observed that $G\alpha_{13}$

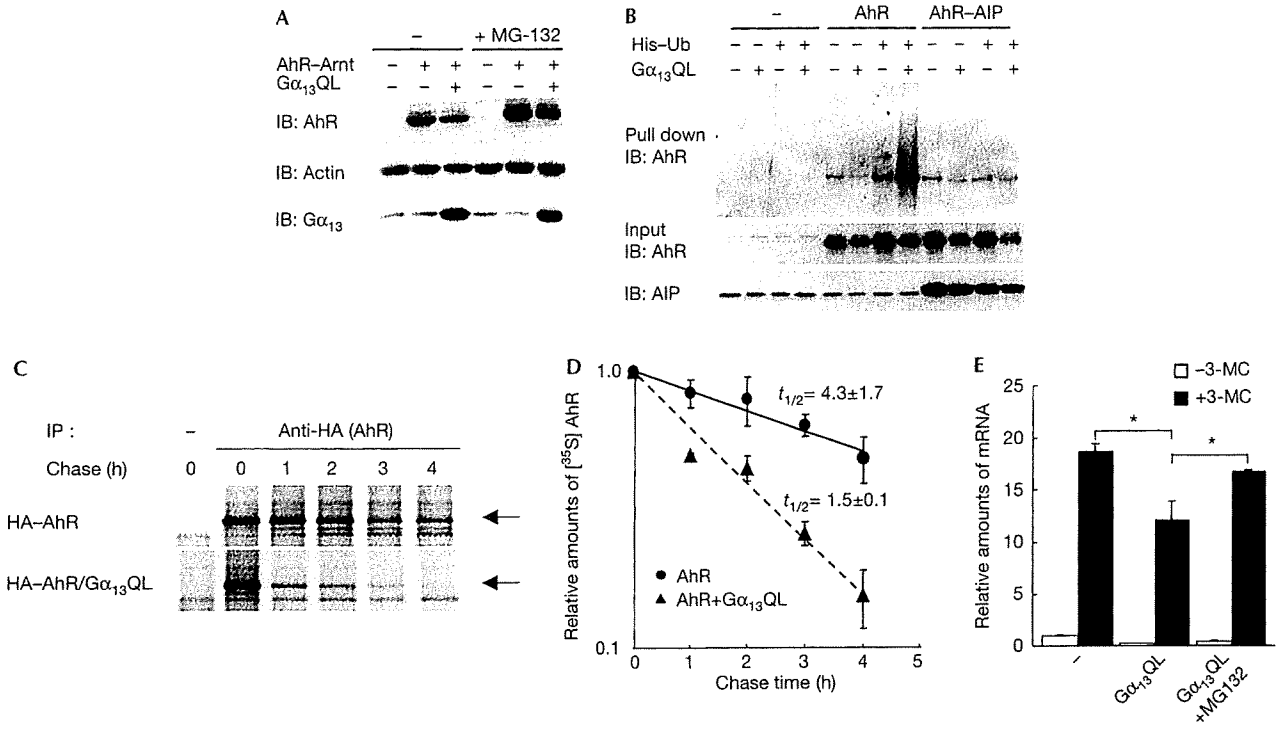

Fig 4 | $G\alpha_{13}$ induces the ubiquitination and degradation of AhR. (**A**) HEK293T cells transfected as indicated were treated with or without 10 μM MG-132 for 4 h. Then, cell lysates were analysed by immunoblot (IB) analysis with the indicated antibodies. (**B**) HEK293T cells expressing $[His]_6$-ubiquitin (Ub), HA-AhR and Myc-AIP with or without $G\alpha_{13}Q226L$ were lysed, and the ubiquitinated proteins were precipitated by Ni-NTA agarose. The ubiquitinated AhR, AhR and AIP in the total lysate were analysed by immunoblot. (**C,D**) HEK293T cells transfected as indicated were tagged metabolically with [^{35}S]-labelled methionine and cysteine for 1 h. Then, the cells were used for pulse-chase analysis. The values of $t_{1/2}$ were obtained from three independent experiments. Arrows indicate immunoprecipitated AhR. (**E**) Hepa1c1c7 cells were transfected as indicated and stimulated with 1 μM 3-MC for 8 h in the presence or absence of 10 μM MG-132. The expression of CYP1A1 was analysed by the quantitative RT-PCR method. 3-MC, 3-methyl cholanthrene; AhR, aryl hydrocarbon receptor; AIP, AhR-interacting protein; HA, haemagglutinin; HEK, human embryonic kidney.

overexpression disturbed the association of AIP with AhR, suggesting that $G\alpha_{13}$ might impede the stabilization of AhR by AIP. We confirmed that the overexpression of $G\alpha_{13}Q226L$ resulted in the downregulation of the AhR protein (Fig 4A, lanes 2 and 3) and that the proteasome inhibitor, MG-132, restored the downregulation of AhR (Fig 4A, lanes 5 and 6). Then, we tested the effect of $G\alpha_{13}$ on the ubiquitination of AhR. HEK293T cells were transfected with AhR and histidine-tagged ubiquitin. Ubiquitinated AhR was precipitated by Ni-agarose and detected by immunoblot. As expected, the ubiquitination of AhR was promoted by $G\alpha_{13}Q226L$ (Fig 4B, lanes 7 and 8). Conversely, the ubiquitination of AhR was suppressed by the overexpression of AIP (Fig 4B, lanes 9–12). Next, to examine whether $G\alpha_{13}$ affects the protein stability of AhR, pulse-chase analysis was performed. The half-life of AhR was about 4.3 h in the absence of $G\alpha_{13}Q226L$. Conversely, when $G\alpha_{13}Q226L$ was coexpressed, AhR was degraded with a half-life of 1.5 h (Fig 4C,D). These data suggest that $G\alpha_{13}$ suppresses the activation of AhR through the destabilization of AhR by the ubiquitin–proteasome pathway. This possibility was also supported by the evidence that the expression of AhR was reduced by $G\alpha_{13}$ expression (Figs 1E,3B,4B). Interestingly, as shown in Fig 1E, overexpression of AIP effectively cancelled the $G\alpha_{13}$-induced reduction of AhR in whole-cell lysate (compare lanes 3 and 4, with lanes 7 and 8), and also in Fig 4B, coexpressed AIP diminished the ubiquitination of AhR accelerated by $G\alpha_{13}$. These results supported our hypothesis that $G\alpha_{13}$ competitively sequesters AIP from the AhR complex and this would be the trigger for $G\alpha_{13}$-induced suppression of activation of AhR. Also, we tested whether inhibition of proteasome is able to cancel the $G\alpha_{13}$-induced suppression of activation of AhR. As shown in Fig 4E, a proteasome inhibitor MG-132 showed the cancellation of the inhibitory effect of $G\alpha_{13}$, suggesting that promoting the proteasome-mediated degradation of AhR is one of the molecular mechanisms by which $G\alpha_{13}$ diminishes ligand-dependent activation of AhR. As shown in Fig 3, $G\alpha_{13}$ induced the ligand-independent nuclear localization of AhR, but did not allow AhR to interact with Arnt. It has been reported that the nuclear-localized AhR is unstable and degraded more rapidly in the absence of Arnt (Roberts & Whitelaw, 1999). This report supports our model that the $G\alpha_{13}$-induced nuclear localization of AhR might be the trigger for the degradation of AhR.

Through our current research, we have also shown that G_q has a potent inhibitory effect on AhR in spite of its weak interacting activity. Several signalling molecules have been reported to regulate the AhR signal. Some of them are activated by

$G\alpha_q$ signalling, including the transcription factor NF-κB (Harper *et al*, 2006). $G\alpha_q$ might affect AhR through these downstream molecules.

The C terminus of HSC70-interacting protein (CHIP) is known as E3 ligase, which contains three TPR motifs and a U-box domain (McDonough & Patterson, 2003), and has been reported to be involved in the ubiquitination of AhR (Lees *et al*, 2003). CHIP might be E3 ubiquitin ligase in the $G\alpha_{13}$-induced degradation of AhR. Here, we propose a new model to explain how the activation of AhR is attenuated by extracellular signals. The determination of which E3 ubiquitin ligase is involved in the $G\alpha_{13}$-induced suppression of AhR activity should be the focus of a future study.

METHODS

Cell culture and transfection. HEK293T, COS-7 and Hepa1c1c7 cells were maintained in Dulbecco's modified Eagle's medium supplemented with 10% FBS and 100 μg/ml kanamycin at 37 °C and 5% CO_2. Transfection into HEK293T and COS-7 cells was performed using the calcium phosphate method. Hepa1c1c7 cells were transfected using Lipofectamine2000 (Invitrogen; Carlsbad, CA, USA).

RNA interference. Annealed siRNA complexes for mouse AIP and firefly luciferase were purchased from Thermo Fisher Scientific Inc. (Waltham, MA, USA). The mixture of siRNA (final concentration, 50 nM) was transfected by using Lipofectamine2000 into 35-mm dishes containing 1×10^5 Hepa1c1c7 cells. At 48 h after transfection, cells were analysed as described in the text. The sequences of siRNA were shown in supplementary Fig 2A online.

Reporter gene analysis. For reporter gene analysis, cells were plated onto a 48-well plate. COS-7 or Hepa1c1c7 cells transfected with the indicated combinations of plasmids, including haemagglutinin–AhR, GST–Arnt, FLAG–$G\alpha_{13}$Q226L, pXRE–luciferase and pEF–RL, were stimulated with 1 μM 3-MC or 10 μM LPA (Sigma-Aldrich; St Louis, MO, USA) for 24 h (reporter gene analysis) or 12 h (RT–PCR). The reporter gene analysis was performed with the Dual Luciferase Assay kit (Promega).

EMSA. The nuclear extracts were mixed with 3 μg of poly (dI-dC; GE Healthcare; Buckinghamshire, England) and a radioactively labelled probe (2×10^4 c.p.m.) in a final volume of 25 μl of EMSA-binding buffer (10 mM HEPES-KOH (pH 7.8), 1 mM EDTA, 5 mM $MgCl_2$, 10% glycerol and 50 mM KCl) and incubated for 20 min at 25 °C. The protein–DNA complex was separated by 4.5% polyacrylamide gel using 0.5 × TGE (12.5 mM Tris, 95 mM glycine and 0.5 mM EDTA) as a running buffer and detected by autoradiography. In several experiments, the AhR or Arnt (H-172; Santa Cruz Biotechnology; Santa Cruz, CA, USA) antibody was added into the reactive mixture. The annealed oligo probe 5′-GATCCGGCTCTTGTCACGCAACTCCGAGCTCA-3′ includes the XRE sequence (shown here underlined). The oligo probe was radioactively labelled by T4-polynucleotide kinase (TOYOBO; Osaka, Japan) with [γ-^{32}P]ATP.

Pulse-chase analysis. For pulse-chase analysis, the transfected HEK293T cells were cultured in DMEM including [^{35}S]methionine and [^{35}S]cysteine for 60 min. Cells were then cultured in DMEM containing 2 mM non-radioactive methionine and cysteine for the indicated periods and collected in 500 μl of RIPA buffer (10 mM Tris–HCl (pH 7.5), 150 mM NaCl, 5 mM EDTA, 1% Triton X-100 and 1% deoxycholate). [^{35}S]-labelled AhR was precipitated with the haemagglutinin antibody, separated by SDS-polyacrylamide gel electrophoresis, and detected by autoradiography.

Supplementary information is available at *EMBO reports* online (http://www.emboreports.org)

ACKNOWLEDGEMENTS

We thank Dr Dirk Bohmann for providing pMT107-[His]$_6$-ubiquitin. This study was supported by grants-in-aid for scientific research from the Ministry of Education, Culture, Sports, Science, and Technology of Japan (17079006).

CONFLICT OF INTEREST

The authors declare that they have no conflict of interest.

REFERENCES

Baba T, Mimura J, Nakamura N, Harada N, Yamamoto M, Morohashi K, Fujii-Kuriyama Y (2005) Intrinsic function of the aryl hydrocarbon (dioxin) receptor as a key factor in female reproduction. *Mol Cell Biol* **25:** 10040–10051

Blatch GL, Lässle M (1999) The tetratricopeptide repeat: a structural motif mediating protein–protein interactions. *Bioessays* **21:** 932–939

Carver LA, Bradfield CA (1997) Ligand-dependent interaction of the aryl hydrocarbon receptor with a novel immunophilin homolog *in vivo*. *J Biol Chem* **272:** 11452–11456

Froidevaux MS, Berg P, Seugnet I, Decherf S, Becker N, Sachs LM, Bilesimo P, Nygard M, Pongratz I, Demeneix BA (2006) The co-chaperone XAP2 is required for activation of hypothalamic thyrotropin-releasing hormone transcription *in vivo*. *EMBO Rep* **7:** 1035–1039

Fujii-Kuriyama Y, Mimura J (2005) Molecular mechanisms of AhR functions in the regulation of cytochrome *P*450 genes. *Biochem Biophys Res Commun* **338:** 311–317

Gilman AG (1987) G proteins: transducers of receptor-generated signals. *Annu Rev Biochem* **56:** 615–649

Harper PA, Riddick DS, Okey AB (2006) Regulating the regulator: factors that control levels and activity of the aryl hydrocarbon receptor. *Biochem Pharmacol* **72:** 267–279

Kaziro Y, Itoh H, Kozasa T, Nakafuku M, Satoh T (1991) Structure and function of signal-transducing GTP-binding proteins. *Annu Rev Biochem* **60:** 349–400

Kazlauskas A, Poellinger L, Pongratz I (2000) The immunophilin-like protein XAP2 regulates ubiquitination and subcellular localization of the dioxin receptor. *J Biol Chem* **275:** 41317–41324

Kurose H (2003) $G\alpha_{12}$ and $G\alpha_{13}$ as key regulatory mediator in signal transduction. *Life Sci* **74:** 155–161

LaPres JJ, Glover E, Dunham EE, Bunger MK, Bradfield CA (2000) ARA9 modifies agonist signaling through an increase in cytosolic aryl hydrocarbon receptor. *J Biol Chem* **275:** 6153–6159

Lees MJ, Whitelaw ML (2002) Effect of ARA9 on dioxin receptor mediated transcription. *Toxicology* **181–182:** 143–146

Lees MJ, Peet DJ, Whitelaw ML (2003) Defining the role for XAP2 in stabilization of the dioxin receptor. *J Biol Chem* **278:** 35878–35888

Lin BC, Nguyen LP, Walisser JA, Bradfield CA (2008) A hypomorphic allele of aryl hydrocarbon receptor-associated protein-9 produces a phenocopy of the AHR-null mouse. *Mol Pharmacol* **74:** 1367–1371

Marty C, Browning DD, Ye RD (2003) Identification of tetratricopeptide repeat 1 as an adaptor protein that interacts with heterotrimeric G proteins and the small GTPase Ras. *Mol Cell Biol* **23:** 3847–3858

McDonough H, Patterson C (2003) CHIP: a link between the chaperone and proteasome systems. *Cell Stress Chaperones* **8:** 303–308

Meyer BK, Petrulis JR, Perdew GH (2000) Aryl hydrocarbon (Ah) receptor levels are selectively modulated by Hsp90-associated immunophilin homolog XAP2. *Cell Stress Chaperones* **5:** 243–254

Meyer BK, Pray-Grant MG, Vanden Heuvel JP, Perdew GH (1998) Hepatitis B virus X-associated protein 2 is a subunit of the unliganded aryl hydrocarbon receptor core complex and exhibits transcriptional enhancer activity. *Mol Cell Biol* **18:** 978–988

Mimura J, Fujii-Kuriyama Y (2003) Functional role of AhR in the expression of toxic effects by TCDD. *Biochim Biophys Acta* **1619:** 263–268

Petrulis JR, Kusnadi A, Ramadoss P, Hollingshead B, Perdew GH (2003) The hsp90 co-chaperone XAP2 alters importin β recognition of the bipartite nuclear localization signal of the Ah receptor and represses transcriptional activity. *J Biol Chem* **278:** 2677–2685

Pollenz RS, Dougherty EJ (2005) Redefining the role of the endogenous XAP2 and C-terminal hsp70-interacting protein on the endogenous Ah receptors expressed in mouse and rat cell lines. *J Biol Chem* **280:** 33346–33356

Roberts BJ, Whitelaw ML (1999) Degradation of the basic helix–loop–helix/Per–ARNT–Sim hoomology domain dioxin receptor via the ubiquitin/proteasome pathway. *J Biol Chem* **274:** 36351–36356

Schmidt JV, Bradfield CA (1996) Ah receptor signaling pathways. *Annu Rev Cell Dev Biol* **12:** 55–89

Sumanasekera WK, Tien ES, Turpey R, Vanden Heuvel JP, Perdew GH (2003) Evidence that peroxisome proliferator-activated receptor α is complexed with the 90-kDa heat shock protein and the hepatitis virus B X-associated protein 2. *J Biol Chem* **278:** 4467–4473

Yamaguchi Y, Katoh H, Mori K, Negishi M (2002) $G\alpha_{12}$ and $G\alpha_{13}$ interact with Ser/Thr protein phosphatase type 5 and stimulate its phosphatase activity. *Curr Biol* **12:** 1353–1358

THE JOURNAL OF BIOLOGICAL CHEMISTRY VOL. 284, NO. 17, pp. 11017–11026, April 24, 2009

SUMO Modification Regulates the Transcriptional Repressor Function of Aryl Hydrocarbon Receptor Repressor*[S]

Received for publication, November 17, 2008, and in revised form, February 27, 2009 Published, JBC Papers in Press, February 27, 2009, DOI 10.1074/jbc.M808694200

Motohiko Oshima[‡§], Junsei Mimura[¶], Hiroki Sekine[‡§], Hiromi Okawa[‡§], and Yoshiaki Fujii-Kuriyama[‡§1]

From the [‡]Center for Tsukuba Advanced Research Alliance and Institute of Basic Medical Sciences, University of Tsukuba, 1-1-1 Tennoudai, Tsukuba 305-8577, Japan, the [¶]Department of Stress Response Science, Hirosaki University Graduate School of Medicine, Hirosaki, Aomori 036-8562, Japan, and [§]Solution Oriented Research for Science and Technology, Japan Science and Technology Agency, 4-1-8 Honcho, Kawaguchi 332-0012, Japan

The aryl hydrocarbon receptor (AhR) repressor (AhRR) inhibits the AhR activity. AhRR acts by competing with AhR for heterodimer formation with the AhR nuclear translocator (Arnt) and preventing the AhR·Arnt complex from binding the xenobiotic-responsive elements. Here, we report that AhRR has three evolutionarily conserved SUMOylation consensus sequences within its C-terminal repression domain and that Lys-542, Lys-583, and Lys-660 at the SUMOylation sites are modified by SUMO-1 *in vivo*. Arginine mutation of the three lysines results in a significant reduction of transcriptional repression activity. SUMOylation of the three lysine residues is important for the interaction between AhRR and ANKRA2, HDAC4, and HDAC5, which are important corepressors for AhRR. Arnt, a heterodimer partner for AhRR, markedly enhanced the SUMOylation of AhRR. AhRR, but not AhR, also significantly enhanced the SUMOylation of Arnt. The SUMOylation of both AhRR and Arnt is important for the efficient transcriptional repression activity of the AhRR/Arnt heterodimer.

The aryl hydrocarbon receptor repressor (AhRR)[2] is a member of the bHLH-PAS (basic helix-loop-helix and the Per-Arnt-Sim) protein superfamily and has a high similarity to AhR in the N-terminal bHLH-PAS A domain (1). The 5′-flanking promoter region of the mouse AhRR gene contains conserved xenobiotic-responsive element (XRE) sequences, and expression of the AhRR gene is induced by binding of the AhR/Arnt heterodimer to these XREs (2). AhRR forms a heterodimer with Arnt, another bHLH-PAS transcription factor, to inhibit AhR-dependent transactivation of the XRE-driven genes; thus, AhRR participates in a negative feedback loop in the AhR signaling pathway (1, 3, 4). Recently, we generated AhRR$^{-/-}$ mice, which show higher than wild type levels of ligand-induced expression of the AhR target gene, *Cyp1a1* mRNA induction in some tissues (5). These mice also displayed a delayed response to skin carcinogenesis caused by benzo[a]pyrene (5). Recent work has also demonstrated that AhRR is a tumor suppressor gene (6); AhRR mRNA is consistently down-regulated in human malignant tissues from different anatomical origins; furthermore, ectopic expression of AhRR in tumor cells resulted in diminished cell growth (7) and reduced angiogenic potential. These observations provide new insight into the still largely unknown physiological functions of AhRR and form the basis for further studies of its mechanisms of action.

We reported previously that AhRR contains a transcriptional repression domain within its C-terminal region (8). Using the C-terminal region of AhRR as bait, we isolated ANKRA2 (ankyrin repeat, family A, 2) by CytoTrap yeast two-hybrid screening. AhRR was also shown to interact with HDAC4 and HDAC5, and these interactions are important for the transcriptional repression activity of AhRR (8).

Small ubiquitin-like modifiers (SUMO-1, SUMO-2, and SUMO-3) belong to a family of ubiquitin-like proteins, which are covalently attached to (or detached from) substrate proteins to regulate their functions. The post-translational modification of proteins by SUMO has been increasingly recognized as an important regulatory mechanism in a diverse range of cellular processes. SUMO precursors are processed by SUMO-specific proteases and activated by an E1 enzyme. The activated SUMO is transferred to the E2 conjugating enzyme Ubc9, which recognizes the SUMOylation consensus sequence ψKXE within target proteins. With the help of E3 ligases such as PIAS, the C-terminal glycine of SUMO is covalently linked to the ϵ-amino group of lysine in the SUMOylation consensus sequence of the target proteins (9, 10).

In contrast to ubiquitylation, SUMOylation has a wide range of substrate-specific functions and acts via multiple mechanisms, including alterations in the subcellular localization of target proteins, protein stability, protein-protein interactions, and protein-DNA binding activities. Many transcription factors are SUMOylated. In many cases, SUMO modification of transcription factors is associated with transcriptional repression through the suppression of transactivation activity or the enhancement of repression activity.

In this study, we report that three lysine residues within the C-terminal repression domain of AhRR can be modified by

* This work was supported in part by a scientific research grant from the Ministry of Health, Labor, and Welfare of Japan and Solution Oriented Research for Science and Technology, Japan Science and Technology Agency.

[S] The on-line version of this article (available at http://www.jbc.org) contains supplemental Fig. S1.

[1] To whom correspondence should be addressed: Center for Tsukuba Advanced Research Alliance, University of Tsukuba, 1-1-1 Tennoudai, Tsukuba, Ibaraki 305-8577, Japan. Tel.: 81-29-853-7323; Fax: 81-29-853-7318; E-mail: ykfujii@tara.tsukuba.ac.jp.

[2] The abbreviations used are: AhRR, aryl hydrocarbon receptor repressor; AhR, aryl hydrocarbon receptor; SUMO, small ubiquitin-like modifier; WT, wild type; EGFP, enhanced green fluorescent protein; XRE, xenobiotic-responsive element; HA, hemagglutinin; m, mouse; Arnt, AhR nuclear translocator; GAL4DBD, GAL4 DNA-binding domain; 3-MC, 3-methyl cholanthrene; PML, promyelocytic leukemia.

SUMO-1, resulting in enhancement of its transcriptional repression activity.

EXPERIMENTAL PROCEDURES

Plasmids—Constructions of pBOSGAL4DBD-AhRR, pBOSHA-AhRR, pBOSFLAG-ANKRA2, pG3TK-Luc, and plasmids encoding HDAC4-FLAG and HDAC5-FLAG was described previously (8). pSG5His-SUMO-1 was generated by fusing full-length human *SUMO-1* cDNA with the His tag sequence and cloning into the expression vector pSG5 (Stratagene). pBOSHA-SUMO-1 and pBOSHA-SUMO-2 were generated by ligating the full-length human *SUMO-1* or *SUMO-2* cDNA with the SmaI site of pBOST7-HA. pBOS-Ubc9 was generated by inserting the EcoRI/SalI fragment of pBSK-mUbc9 into the pEFBOS vector (11) cleaved with EcoRI/SalI. pCMV3xFLAG-AhRR was constructed by ligating the blunt-ended EcoRI/SalI fragment from pBSK-mAhRR with the blunt-ended p3xFLAG-CMV-10 (Sigma). AhRR was cleaved from pBSK-AhRR (8) with EcoRI/XhoI, blunt-ended, and subsequently inserted into the EGFP-C3 vector, which was cut with SmaI to generate pEGFP-AhRR. pBOS-AhR, pBOS-Arnt, and pXRE4TK-Luc were described previously (1). To construct pBOSHA-AhR and pBOSHA-Arnt, pBSK-mAhR and pBSK-mArnt (1) were digested with HindIII/XbaI and NcoI/BamHI, respectively, and the blunt-ended fragments of mAhR and mArnt were ligated with the SmaI site of pBOST7-HA. pBOS3xFLAG-Arnt was described previously (12). Single, double, or triple amino acid mutations in AhRR (K542R, K583R, K660R) or Arnt (K245R) were generated using the QuikChange site-directed mutagenesis kit (Stratagene).

Cell Culture and Transfection—COS-7, Hepa-1c1c7 (Hepa-1), and HeLa cells were maintained, respectively, in high or low glucose Dulbecco's modified Eagle's medium (Sigma) supplemented with 10% fetal bovine serum (Sigma) and penicillin/streptomycin (Invitrogen) under 5.0% CO_2 at 37 °C. Transfection was performed using Lipofectamine™ (Invitrogen).

Luciferase Assay—Hepa-1, COS-7, or HeLa cells (5.0×10^4 cells/well) were grown in 24-well dishes for 24 h and transfected with the expression plasmids indicated in the figure legends, such as pG3TK-Luc or pXRE4TK-Luc, and the expression plasmids for sea pansy luciferase as an internal control. Cells transfected with pXRE4TK-Luc were treated with 2 μM 3-MC or Me_2SO for 12 h. Forty eight h after transfection, the cells were harvested, and luciferase was quantified using the Dual-Luciferase reporter assay system (Promega). Expressed firefly luciferase activity was normalized to the cotransfected sea pansy luciferase activity, which was used as a standard.

Co-immunoprecipitation and Immunoblot Analysis—The transfected COS-7 cells were lysed in radioimmune precipitation assay buffer for immunoprecipitation with the anti-HA antibody or in FLAG buffer for immunoprecipitation with the anti-FLAG antibody; buffer contained protease inhibitor mixture (Roche Applied Science) and 20 mM *N*-ethylmaleimide to preserve the SUMOylation. Whole cell lysates were used for immunoblot analysis either directly or after immunoprecipitation. Immunoprecipitation with anti-FLAG M2 agarose (Sigma) or anti-HA agarose (Sigma) was performed for 12 h, and the immunoprecipitates were washed according to the published procedure for immunoblot analysis. Immunoblot analysis was performed using anti-FLAG (Sigma), anti-HA (Sigma), anti-SUMO-1 (ALEXIS), anti-Arnt (13), and anti-AhRR antibodies (8).

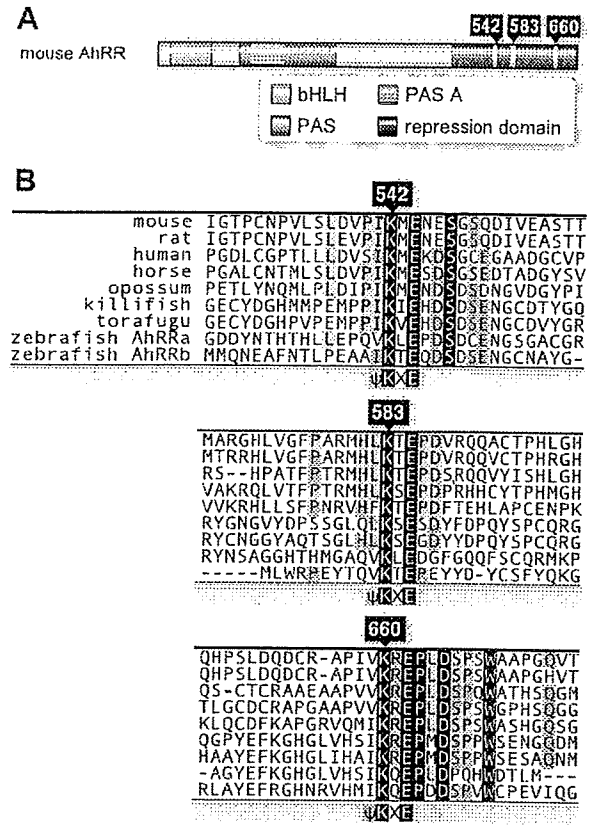

FIGURE 1. **Three conserved SUMOylation sequences in the C-terminal repression domain of AhRR.** *A*, schematic representation of the full-length 701-amino acid mouse AhRR. The characterized domains represented are the basic helix-loop-helix (*bHLH*), Per-Arnt-Sim (*PAS*), and repression domains. Three putative SUMOylation sites are located within the repression domain, with the target lysine residues indicated. *B*, alignments of C-terminal regions of AhRR, including three SUMOylation sites found in mouse, rat, human, horse, opossum, killifish, torafugu, and zebrafish. Conserved amino acids are highlighted in *black*, and the conserved SUMOylation sites and lysine residues are indicated.

RESULTS

Three Evolutionarily Conserved SUMOylation Sites in AhRR—To gain insight into the function of AhRR, we inspected the amino acid sequence of mouse AhRR to identify structural motifs for potential covalent modification sites. We found three SUMOylation consensus sequences at amino acid positions 542, 583, and 660 (Fig. 1*A*). All of these sequences are located within the repression domain of AhRR (8). Three SUMOylation sites are well conserved across a broad range of vertebrate species, including mammals and fish (Fig. 1*B*). Other AhRR C-ter-

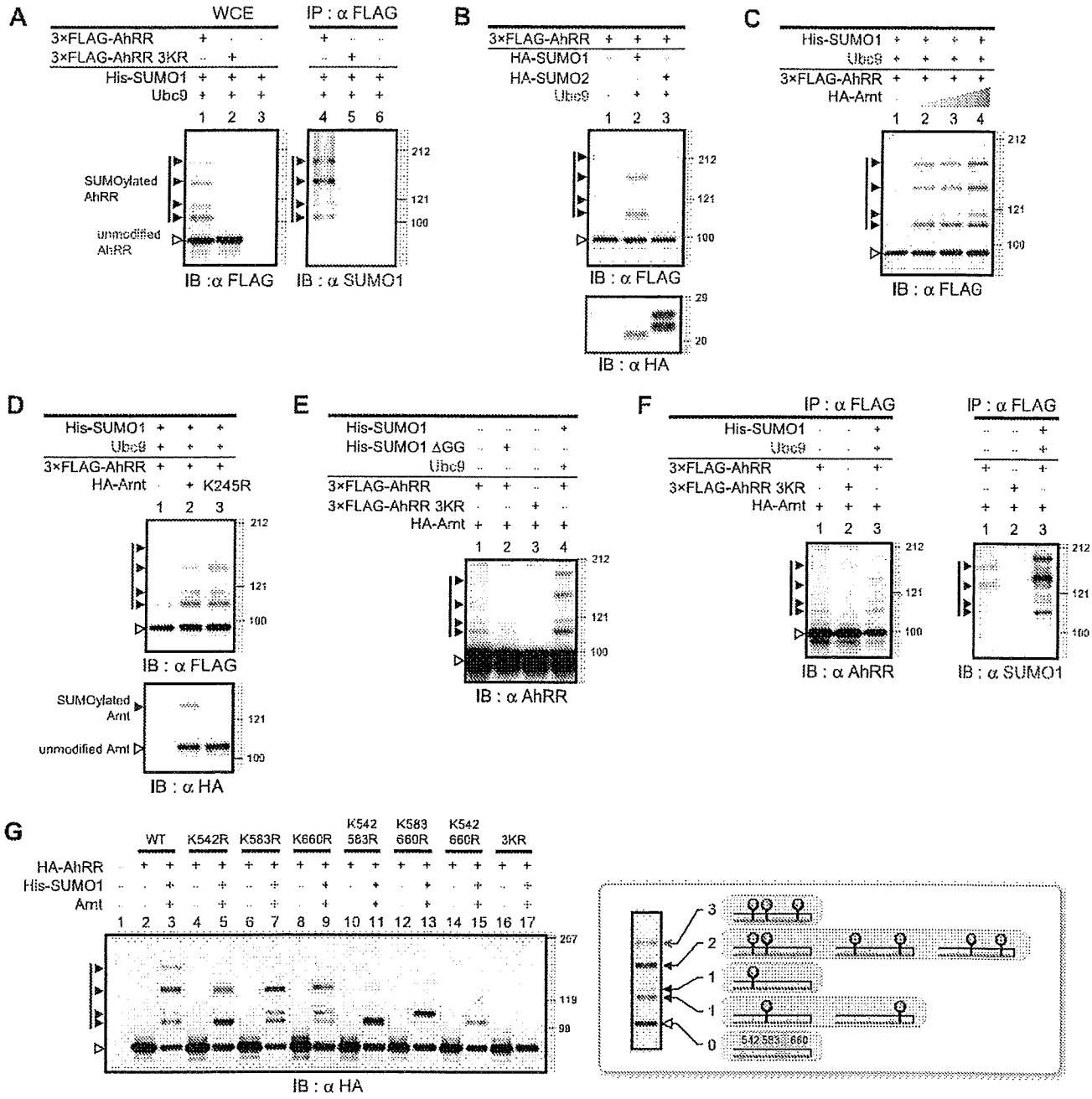

FIGURE 2. **Lysines at 542, 583, and 660 amino acids of AhRR are modified by SUMO-1.** *A* and *F*, COS-7 cells were cotransfected with indicated plasmids, and whole cell extracts (*WCE*) were prepared 48 h after transfection and immunoprecipitated (*IP*) with anti-FLAG antibodies. Immunoprecipitates were analyzed by immunoblotting (*IB*) with the indicated antibodies. Crude lysates were analyzed by immunoblotting to control protein expressions. *B–E* and *G*, COS-7 cells were cotransfected with the indicated expression plasmids. Cell extracts were prepared 48 h after transfection and analyzed by immunoblotting with the indicated antibodies as described above. *Black* and *white arrowheads* indicate SUMOylated or unmodified AhRR, respectively. In *G*, the *right panel* presents the SUMOylation sites and mobility of AhRR.

minal regions have no obvious sequence conservation, suggesting that the putative SUMOylation motifs play an important role in AhRR transcriptional repression activity.

Lysines at Amino Acids 542, 583, and 660 of AhRR Are Modified by SUMO-1—To examine whether these potential SUMO modification sites are actually SUMOylated *in vivo*, we replaced the three conserved lysines with arginines to create the AhRR 3KR mutant. COS-7 cells were cotransfected with expression plasmids for 3xFLAG-AhRR WT or 3xFLAG-AhRR 3KR, along with His-SUMO-1 and Ubc9. In addition to a band for AhRR (~80 kDa), Western blotting using anti-FLAG antibodies detected four bands with slower mobilities when 3xFLAG-AhRR WT was cotransfected, presumably corresponding to various SUMOylated AhRRs (Fig. 2*A*, *left panel*). These bands were also detected without adding Ubc9, although bands were weaker than those in the presence of added Ubc9 (data not shown). In contrast, when 3xFLAG-AhRR 3KR was cotransfected, no slower mobility bands were observed. When cell

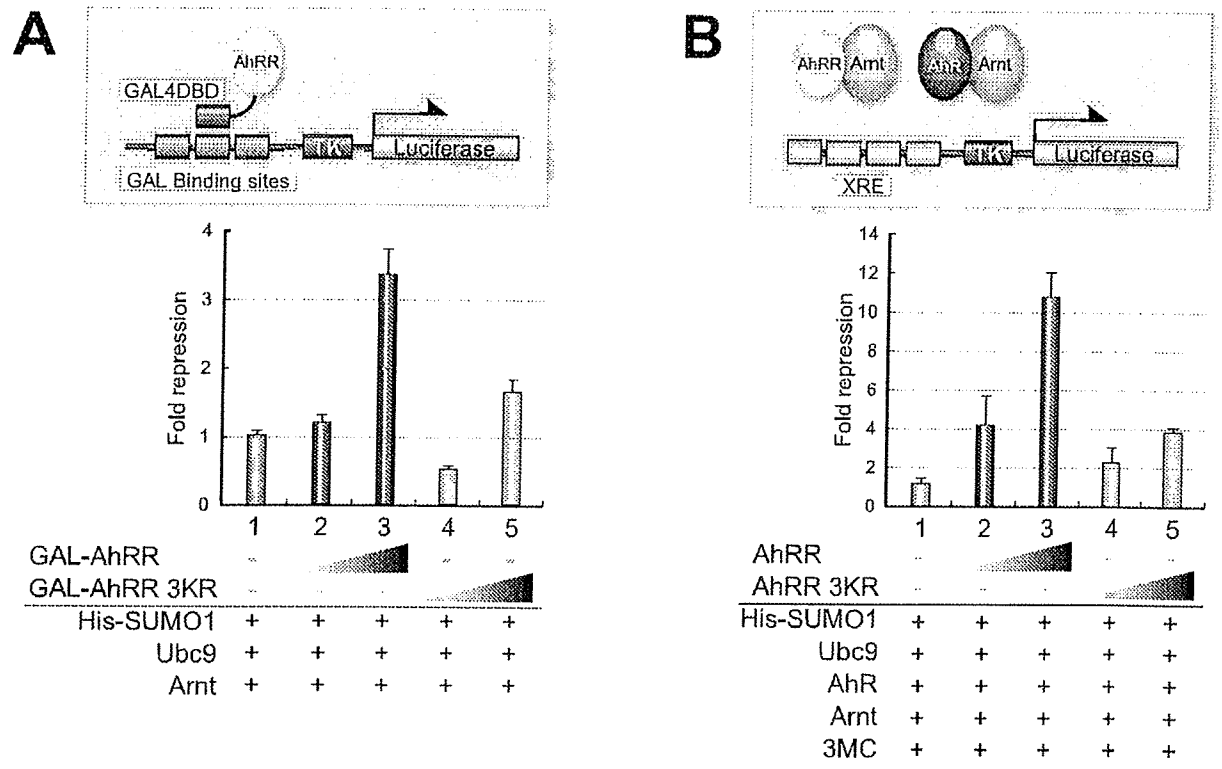

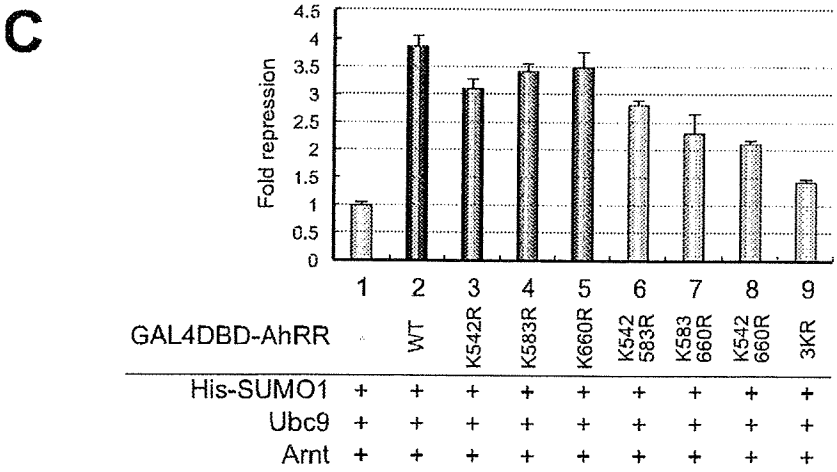

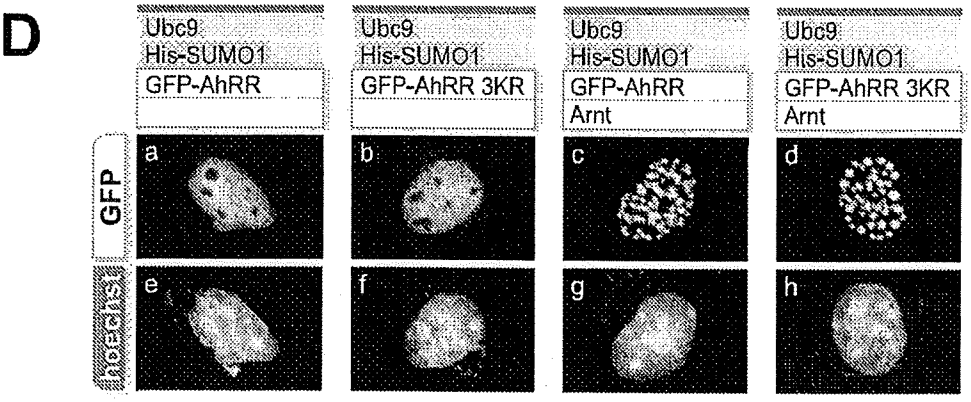

extracts were immunoprecipitated with anti-FLAG antibodies, followed by Western blotting using anti-SUMO-1 antibodies, four higher molecular weight bands with the same mobilities were detected (Fig. 2*A*, *right panel*). These results indicate that AhRR is actually SUMOylated *in vivo*, at Lys-542, Lys-583, and Lys-660.

We further examined whether these lysines were also modified by SUMO-2, but when the SUMO-2 plasmid was cotransfected, no modified product of AhRR was observed (Fig. 2*B*). We detected a doublet band of SUMO-2 that was also observed in other reports overexpressing SUMO-2 (14, 15), although the reason is not clear. One possible explanation is that a higher molecular weight band corresponds to immature SUMO-2, which produced the mature SUMO-2 (lower band) by cleaving C-terminal 11 amino acids with SUMO-specific proteases (SENPs) (16). Likewise, addition of any of the PIAS family proteins, which are well characterized SUMO E3 ligases, did not result in increased SUMOylation of AhRR (data not shown). Taken together, these results indicate that AhRR is specifically modified by SUMO-1.

We next investigated whether the heterodimer partner Arnt affects the SUMOylation of AhRR. Arnt is also modified by SUMO-1 (17), and we were interested to know how the SUMOylation of each AhRR and Arnt affects that of the other. As shown in Fig. 2*C*, addition of Arnt significantly enhanced the SUMOylation of AhRR in a dose-dependent manner. Next, to examine whether SUMOylation of Arnt is necessary for enhancement of AhRR SUMOylation, we transfected cells with a plasmid expressing the Arnt K245R mutant plasmid; we observed no difference in AhRR SUMOylation regardless of whether the Arnt WT or K245R mutant was expressed (Fig. 2*D*). These results indicate that heterodimer formation between Arnt and AhRR, but not Arnt SUMOylation, enhances the SUMOylation of AhRR.

Then, we tested whether AhRR was SUMOylated by an endogenous SUMOylation system. When AhRR was expressed in COS-7 cells without exogenous SUMO-1 and Ubc9, four bands, corresponding to the SUMOylated AhRR bands, were also observed (Fig. 2*E*). Bands were of slightly lower mobility than the His-SUMO-1-modified AhRR because of the His tag (Fig. 2*E*, *lanes 1* and *4*). These bands were decreased in intensity when the dominant-negative SUMO-1 mutant with deletion of C-terminal GG residues was cotransfected and disappeared when AhRR 3KR was expressed (Fig. 2*E*, *lanes 2 and 3*). Cell extracts of AhRR-transfected COS-7 cells were immunoprecipitated with anti-FLAG antibodies, followed by Western blotting using anti-SUMO-1 antibodies, and four SUMOylated bands were detected (Fig. 2*F*). These results showed that AhRR was also SUMOylated by the endogenous SUMOylation system.

There are three putative SUMOylation sites in the AhRR amino acid sequence, and four SUMOylated bands were detected in the SUMOylation experiment. We were interested to investigate which sites are actually SUMOylated. We generated arginine mutations in the three lysine residues, either alone or in combination, to identify the SUMOylated bands of AhRR. As shown in Fig. 2*G*, SUMOylated AhRR bands with different mobilities were observed when AhRRs with different Lys-to-Arg mutations were expressed. From the electrophoretic mobilities and the sites of Lys-to-Arg replacement, we were able to attribute the bands to the specifically SUMOylated AhRR species shown in Fig. 2*G*. Taken together, these results showed that AhRR was mono-, di-, and tri-SUMOylated on Lys-542, Lys-583, and Lys-660, and all of these SUMOylations were significantly enhanced when Arnt was coexpressed with AhRR.

SUMO Modification of AhRR Is Important for Its Efficient Transcriptional Repression Activity—Because SUMOylation usually increases the activity of transcriptional repressors, we next examined the effects of SUMOylation on the function of AhRR as a transcriptional repressor. First, we performed a reporter assay using the luciferase gene under the control of the thymidine kinase promoter ligated with GAL4-binding sites (3xGAL-TK-Luc). Transcriptional repression activity of AhRR fused with the GAL4 DNA-binding domain (GAL4DBD) was assessed by measuring the luciferase gene expression driven by the thymidine kinase promoter. AhRR WT repressed the luciferase activity dose-dependently, whereas the 3KR mutant of AhRR significantly reduced the repressive activity compared with the WT (Fig. 3*A*). Expression level of AhRR WT and 3KR were normalized using Western blot analysis (data not shown). Next, we used a luciferase reporter gene driven by four tandemly repeated XREs to assess the repression activity of AhRR. AhRR WT repressed the luciferase expression driven by the XRE sequence to a greater degree than AhRR 3KR (Fig. 3*B*). For Fig. 3 (*A* and *B*), essentially the same results were also observed when SUMO-1 and Ubc9 were not exogenously expressed using HeLa cells (supplemental Fig. S1, *A* and *B*, *lanes 1–3*), indicating that endogenous SUMOylation activity is sufficient for AhRR repression activity. These results indicate that the SUMOylation of AhRR is important for its transcriptional repression activity.

To determine the contribution of each of the three lysines to the repressive activity of AhRR, the GAL4 reporter assay was performed using the mutant AhRR-GAL4DBD fusion genes with the Lys-to-Arg mutations in all three lysine positions,

FIGURE 3. **SUMO modification sites of AhRR and their effects on its transcriptional repression activity.** *A*, shown is the transcriptional repression activity of AhRR WT and 3KR. Hepa-1 cells were transiently transfected with the expression plasmids for GAL4DBD-AhRR WT or 3KR, His-tagged SUMO-1, Ubc9, Arnt, and GAL-TK-Luc reporter gene containing three GAL-binding sites. Cell extracts were prepared 48 h after transfection and used for luciferase assays. The -fold repression is relative to the reporter gene alone. *B*, HeLa cells were transiently transfected with the expression plasmids for AhRR WT or 3KR, His-tagged SUMO-1, Ubc9, AhR, Arnt, and the 4xXRE-TK-Luc reporter gene containing four XREs. After 48 h of transfection, cells were treated with 2 μM of 3-MC or Me_2SO; 24 h later, cell extracts were prepared and used for luciferase assays. *C*, Hepa-1 cells were transiently transfected with the expression plasmids for GAL4DBD-AhRR WT; 3KR or AhRR with Lys-to-Arg mutation(s) of each of the three lysines, either alone or in combination; His-tagged SUMO-1, Ubc9, Arnt, and GAL-TK-Luc reporter gene containing three GAL-binding sites. Cell extracts were prepared 48 h after transfection and used for luciferase assays. *D*, the subnuclear distribution of EGFP-AhRR is not changed in the SUMOylation mutant. Hepa-1 cells were transfected with expression plasmids of EGFP-AhRR WT or 3KR, His-tagged SUMO-1, and Ubc9, with or without Arnt. After 48 h of transfection, cells were incubated with Hoechst DNA stain (*lower panels*), and fluorescence images were taken (*upper panels*).

either alone or in combination. As shown in Fig. 3C, the SUMOylation of each lysine residue contributes similarly to the repression activity of AhRR. These results indicate that SUMO-1 modification of Lys-542, Lys-583, and Lys-660 more or less contribute equally to the transcriptional repression activity of AhRR.

SUMOylation of AhRR Is Required for Interaction of AhRR with Corepressor Components—SUMO modification often regulates the subcellular localization of the target proteins. To examine whether SUMO modification affects nuclear localization of AhRR, we transfected Hepa-1 cells with EGFP-AhRR WT or EGFP-AhRR 3KR and observed their subcellular distributions using fluorescence microscopy. Both EGFP-AhRR WT and EGFP-AhRR 3KR gave a similar diffuse nuclear localization pattern (Fig. 3D, *panels a* and *b*). In contrast, coexpression of Arnt markedly changed the subcellular localization of both proteins to a speckled distribution pattern (Fig. 3D, *panels c* and *d*), with fewer than 40% of the transfected cells retaining a diffuse pattern. This speckled localization pattern is consistent with the Arnt localization pattern (17). The same results were also observed when SUMO-1 and Ubc9 were not exogenously expressed (data not shown). These results indicate that SUMO-1 modification of AhRR does not affect subcellular localization of AhRR, whereas Arnt alters the subnuclear localization of AhRR to the speckled pattern. SUMO modification is also known to play a key role in protein-protein interaction. Previously, we demonstrated that the C-terminal repression domain, which carries the three SUMO-1 modified lysines, interacts with ANKRA2, HDAC4, and HDAC5; these interactions are important for the repression activity of AhRR. Therefore, we examined whether the SUMOylation of AhRR affects the interaction with ANKRA2, HDAC4, and HDAC5. COS-7 cells were transfected with the HA-tagged AhRR WT or 3KR mutant, along with FLAG-tagged ANKRA2, HDAC4, or HDAC5. The cell extracts prepared from the transfected cells were immunoprecipitated with an anti-HA antibody. ANKRA2 was co-immunoprecipitated with AhRR WT, and HDAC4 was coprecipitated only when ANKRA2 was coexpressed (Fig. 4A, *left* and *right panels, lanes 2* and *4*), consistent with the previous report (8). However, when the HA-tagged mutant AhRR 3KR was transfected instead of AhRR WT, immunoprecipitates with an anti-HA antibody detected only a small amount of ANKRA2 and HDAC4 (Fig. 4, *A, left* and *right panels, lane 3*, and *C*), indicating that SUMOylation of AhRR is necessary for efficient interaction with ANKRA2 and HDAC4. As expected, HDAC5 was co-immunoprecipitated with AhRR WT even in the absence of ANKRA2 (Fig. 4B, *left and right panels, lanes 2* and *4*), but binding of HDAC5 with AhRR 3KR was much reduced (Fig. 4B, *left* and *right panels, lane 3*, and *C*). Taken together, these results show that the SUMOylation of AhRR is necessary for efficient interaction with ANKRA2, HDAC4, and HDAC5, resulting in its increased transcriptional repression activity.

AhRR, but Not AhR, Enhances SUMO-1 Modification of Arnt—Arnt forms a heterodimer with AhRR, colocalizes with AhRR in the nucleus, and enhances SUMOylation of AhRR (Figs. 2C and 3D). Arnt was previously reported to be SUMOylated, and SUMOylation of Arnt suppresses GAL4DBD-Arnt-mediated transactivation through dissociation from PML (17). Next, we

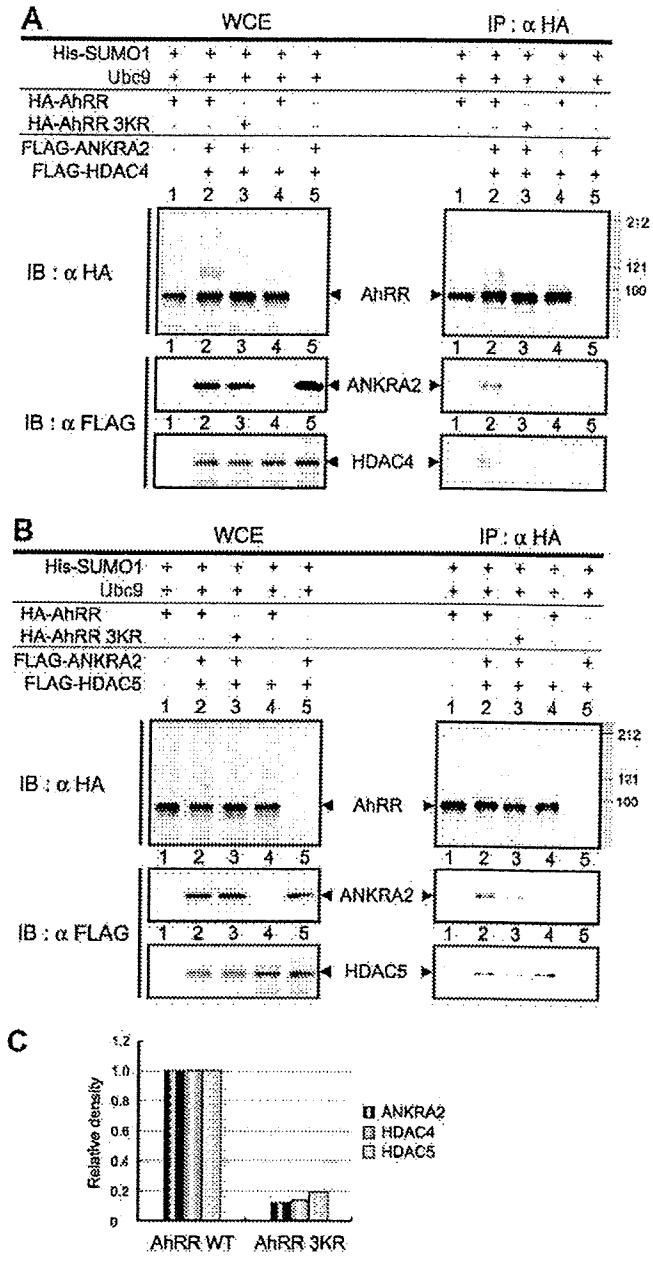

FIGURE 4. **Interaction of SUMO-1-modified AhRR with ANKRA2, HDAC4, and HDAC5.** *A* and *B*, COS-7 cells were cotransfected with expression plasmids for HA-tagged AhRR WT or 3KR, His-tagged SUMO-1, and Ubc9, with or without FLAG-tagged ANKRA2 and FLAG-tagged HDAC4 for *A*, or FLAG-tagged HDAC5 for *B*. Whole cell extracts (*WCE*) were prepared 48 h after transfection and immunoprecipitated (*IP*) with anti-HA antibodies. Immunoprecipitates were analyzed by immunoblot (*IB*) with the indicated antibodies (*B, right panels*). Crude lysates were analyzed by immunoblot to control for protein expression (*B, left panels*). *C*, the relative densities of the ANKRA2, HDAC4, and HDAC5 bands, which were co-immunoprecipitated with either AhRR WT or 3KR, were calculated with NIH Image software. Values are relative to AhRR WT.

examined whether AhRR or AhR affects the SUMO modification of Arnt. Plasmid 3xFLAG-tagged Arnt was transiently expressed in COS-7 cells, together with HA-tagged AhRR or HA-tagged AhR, and the SUMOylated Arnt was examined by Western blotting using an anti-Arnt antibody. Although SUMO-1-modified Arnt was barely detected in the absence of AhRR, SUMO-1-modified Arnt was significantly increased in a

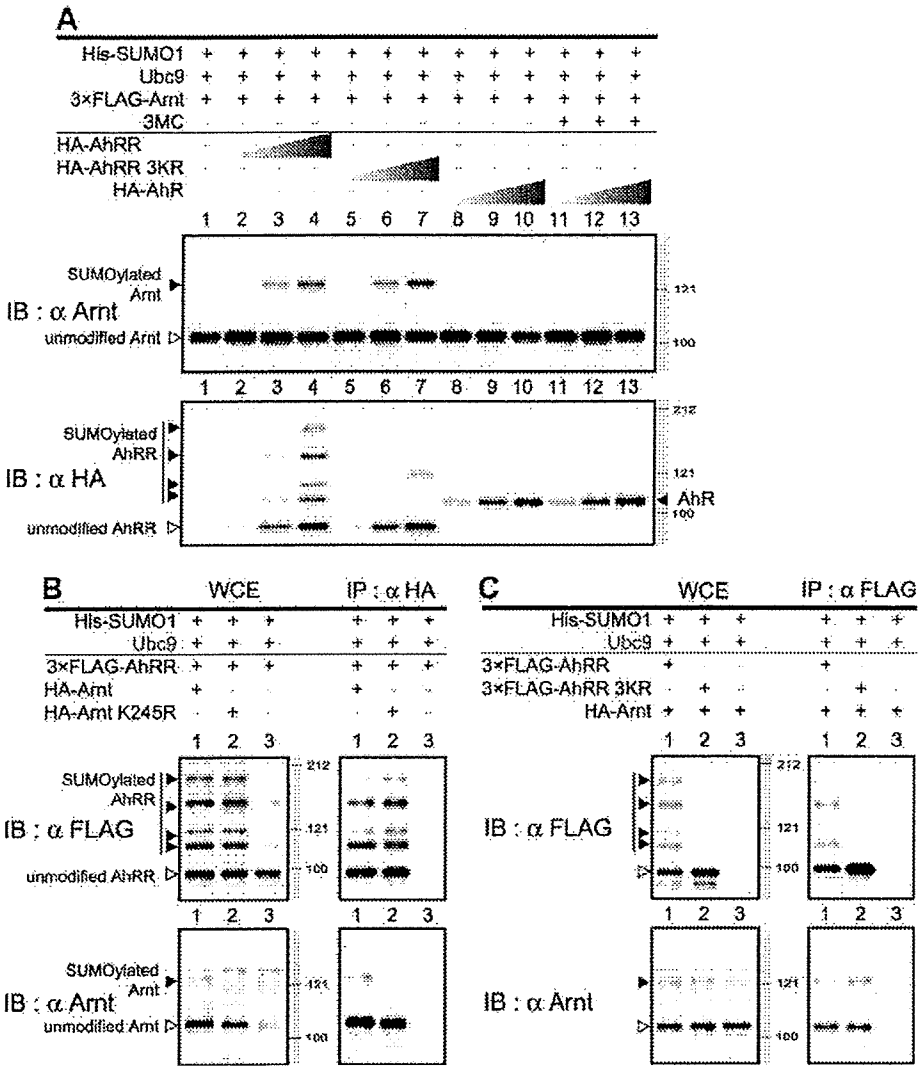

FIGURE 5. **AhRR, but not AhR, and Arnt mutually stimulate one another's SUMO-1 modification.** *A*, COS-7 cells were cotransfected with expression plasmids for HA-tagged AhRR WT or 3KR or HA-tagged AhR, 3xFLAG-tagged Arnt, His-tagged SUMO-1, and Ubc9. After 48 h of transfection, cells for *lanes 11–13* were treated with 2 μM of 3-MC or Me_2SO; 24 h later, whole cell extracts (*WCE*) were prepared and analyzed by immunoblot (*IB*) using the indicated antibodies. *B and C*, COS-7 cells were cotransfected with the indicated expression plasmids. Cell extracts were prepared 48 h after transfection and immunoprecipitated (*IP*) with the indicated antibodies. Immunoprecipitates were analyzed by immunoblot with the indicated antibodies. Crude lysates were analyzed by immunoblot to control for protein expression. *Black* and *white arrowheads* indicate SUMOylated or unmodified AhRR, respectively.

dose-dependent manner upon addition of AhRR (Fig. 5*A*, *lanes 1–4*). The same enhancing effect was observed when AhRR 3KR was cotransfected (Fig. 5*A*, *lanes 5–7*). Therefore, regardless of its SUMOylation, AhRR is necessary for enhancement of Arnt SUMOylation. AhR is also a partner molecule of Arnt for heterodimer formation. We were interested in examining how AhR affects the SUMO modification of Arnt. When HA-tagged AhR was coexpressed with Arnt, no enhancement in the SUMOylation of Arnt was observed, even when the ligands of AhR were added (Fig. 5*A*, *lanes 8–13*). Thus, AhRR and Arnt mutually enhance the SUMOylation of their partner molecules, which may result in enhancement of the repression activity of the AhRR/Arnt heterodimer.

At the same time, these observations raised the question of whether these SUMOylations affect the interaction between AhRR and Arnt. To address this question, COS-7 cells were transfected with expression plasmids for 3xFLAG-tagged AhRR or 3xFLAG-tagged AhRR 3KR, together with HA-tagged Arnt WT or HA-tagged Arnt K245R. Cell extracts were prepared from the transfected cells and immunoprecipitated with anti-HA or anti-FLAG antibodies. No effect of SUMOylation was observed on the interaction between AhRR and Arnt (Fig. 5, *B* and *C*, *lanes 1* and *2*).

SUMOylation of Both AhRR and Arnt Is Important for Repressor Activity of the AhRR·Arnt Complex—We next assessed the potential effects of the SUMOylated Arnt on the repressor activity of the AhRR/Arnt heterodimer. Hepa-1 cells were transfected with expression plasmids for GAL4DBD-fused Arnt WT or K245R, together with His-SUMO-1 and Ubc9, and either of AhR, AhRR WT, or 3KR. GAL4DBD-Arnt WT showed an autonomous transactivation activity, and addition of AhR enhanced this transactivation (Fig. 6*A*, *lanes 1–3*). When non-SUMOylation mutant Arnt K245R was added, there was no difference in transactivation activity from Arnt WT, in agreement with the observation in Fig. 5*A* that Arnt was barely SUMOylated under these conditions (Fig. 6*A*, *lanes 2–5*). This result is also consistent with the previous report that the SUMOylation of Arnt did not affect the transactivation activity of AhR/Arnt or Hif-1α/Arnt (17). When we added AhRR WT, the luciferase expression was remarkably reduced, whereas the addition of AhRR 3KR inhibited the expression of luciferase activity to a lesser extent, with the residual luciferase activity significantly higher than with the wild type AhRR (Fig. 6*A*, *lanes 6* and *7*). This tendency was more remarkable when both non-SUMOylation mutants of AhRR and Arnt were used (Fig. 6*A*, *lane 9*). Next, to further assess the importance of SUMOylation of the AhRR/Arnt heterodimer for its repressor activity, we used a luciferase reporter gene driven by four tandemly repeated XREs. As shown in Fig. 6*B*, the result was almost the same as that as shown in Fig. 6*A*. These experiments were also performed without added SUMO-1 and Ubc9 using HeLa cells, which showed essentially

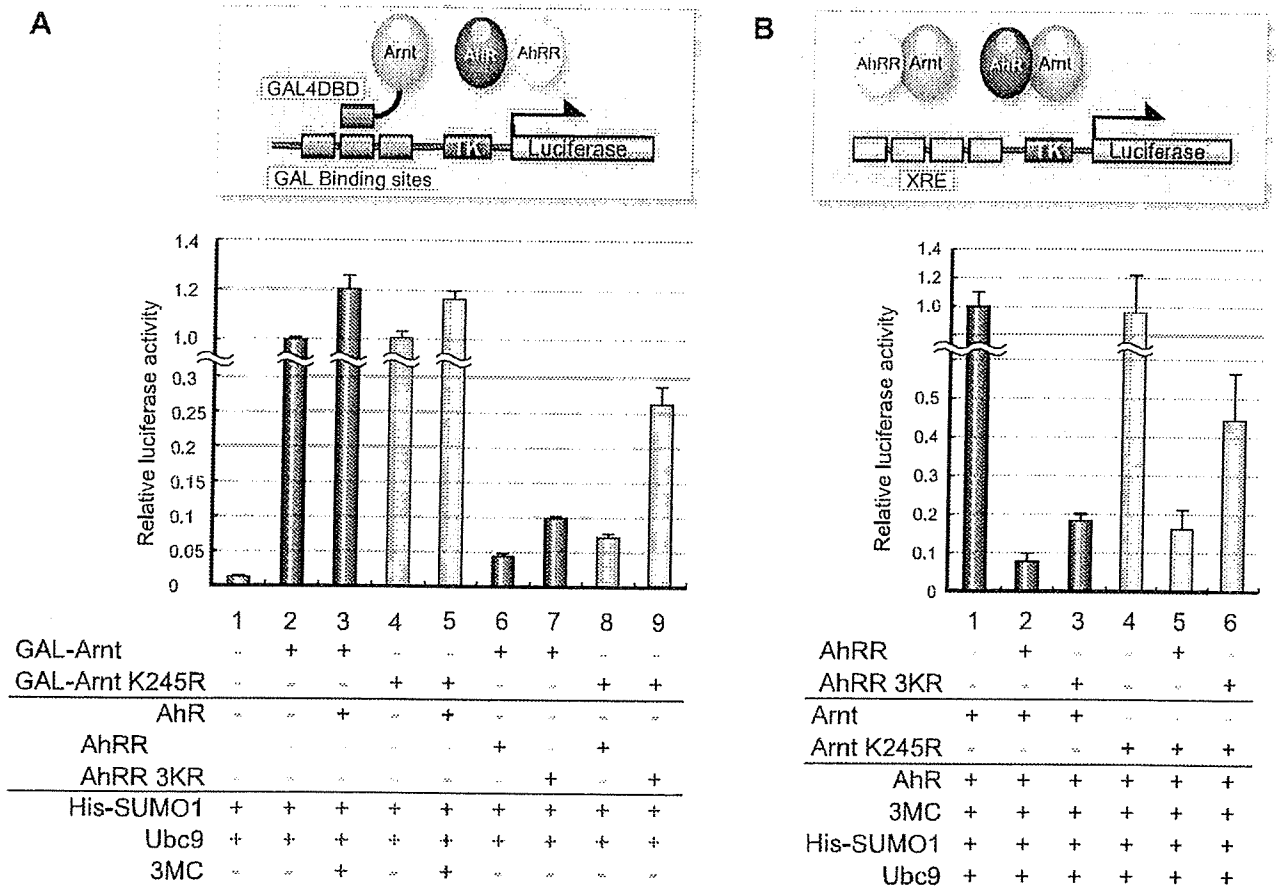

FIGURE 6. **SUMOylation of both AhRR and Arnt is important for the repression activity of the AhRR·Arnt complex.** SUMOylation sites of both AhRR and Arnt are important for the transcriptional repression activity of the AhRR·Arnt complex. *A*, Hepa-1 cells were transiently transfected with the expression plasmids for GAL4DBD-Arnt WT or K245R, AhRR WT or 3KR or AhR, His-tagged SUMO-1, Ubc9, and the GAL-TK-Luc reporter gene containing three GAL-binding sites. After 48 h of transfection, cells for *lanes 3* and *5* were treated with 2 μM of 3-MC or Me_2SO; 24 h later, cell extracts were used for luciferase assays. Luciferase activities are shown as values relative to *lane 2*. *B*, COS-7 cells were transiently transfected with the expression plasmids for Arnt WT or K245R, AhRR WT, 3KR, or AhR, His-tagged SUMO-1, Ubc9, and 4xXRE-TK-Luc reporter gene containing four XRE sequences. After 48 h of transfection, cells were treated with 2 μM of 3-MC or Me_2SO; 24 h later, cell extracts were prepared and used for luciferase assays. Luciferase activities are shown as values relative to *lane 1*.

the same results (supplemental Fig. S1*B*). Taken together, these results show that SUMOylation of both AhRR and Arnt is important for the efficient repressor activity of the AhRR/Arnt heterodimer (Fig. 7).

DISCUSSION

When amino acid sequences of the C-terminal region of AhRR were compared among mammals and fish, three SUMOylation sites including minimal adjacent sequences were revealed to be distinctly conserved (Fig. 1*B*), suggesting that these sequences are involved in some fundamental biological processes. A newly reported composite motif named PDSM (phosphorylation-dependent SUMOylation motif), which contains the SUMO consensus sequence with an adjacent proline-directed phosphorylation site (ψ*KXEXXX*SP) (18–23), undergoes phosphorylation-dependent SUMOylation in many transcription factors, including heat shock proteins (HSPs), peroxisome proliferator-activated receptor γ, MEF2, and GATA-1. Accelerated SUMOylation of these factors by phosphorylation enhances the repression of transcriptional activity. The SUMOylation site at Lys-660 in mouse AhRR, which is well conserved across species, seems to resemble the SUMO consensus sequence accompanying the proline-directed phosphorylation (ψ*KXEXXX*SP), but its functional analysis remains to be seen.

All of the conserved SUMOylation sites of AhRR were found to be SUMOylated more or less equally in our *in vivo* cell culture system. These SUMOylations in AhRR were significantly enhanced by the presence of Arnt, a partner molecule of the AhRR/Arnt heterodimer. Likewise, Arnt was reported previously to be SUMOylated at Lys-245 (17); this SUMOylation was also stimulated by AhRR, but not by AhR, another partner molecule of the transcription-active heterodimer AhR/Anrt. Thus, one of the partner molecules of the AhRR·Arnt repressor complex mutually enhances the SUMOylation of the other (Figs. 2*C* and 5*A*). The PIAS proteins are members of a well characterized SUMO E3 ligase family, consisting of PIAS1, PIASxα, PIASxβ, PIASγ, and PIAS3. However, none of the family members added into the cultured cells could enhance the SUMOylation of AhRR (data not shown). Unlike ubiquitin E3 ligases, apparently structurally unrelated proteins can serve as SUMO E3 ligases, providing a scaffold bridging between Ubc9 and

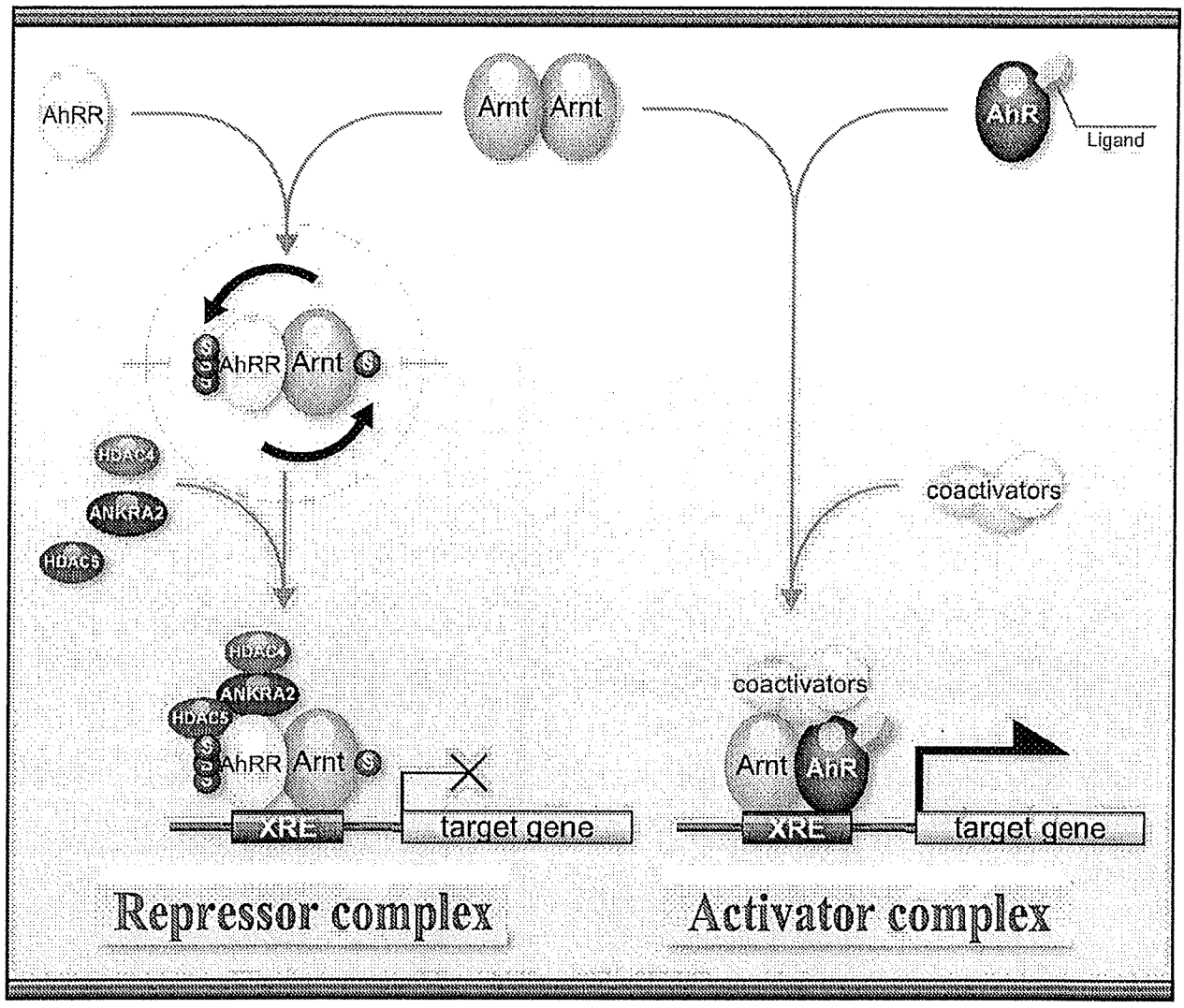

FIGURE 7. **Proposed model for the transcriptional regulation mechanism of the AhR/Arnt activator complex and the AhRR/Arnt repressor complex.** Unmodified Arnt forms a heterodimer with AhR and recruits coactivators such as CBP/p300 to form the transcriptional activator complex. Meanwhile, Arnt forms a heterodimer with AhRR, which significantly enhances SUMOylation of both proteins. SUMOylated AhRR recruits corepressors ANKRA2, HDAC4, and HDAC5 to form the transcriptional repressor complex.

SUMOylation substrates. Whereas the PIAS family apparently plays no role in AhRR modification, Arnt could significantly enhance SUMOylation of AhRR, and the reverse is true with respect to Arnt SUMOylation. Because both AhRR (data not shown) and Arnt (17) interact with Ubc9 and their partner molecules, SUMOylation substrates, it is reasonable to consider that AhRR and Arnt serve as the SUMO E3 ligase to each other. This could be substantiated experimentally by *in vitro* reconstitution of SUMOylation. Interestingly, it has recently been reported that AhR is able to act as an E3 ubiquitin ligase to estrogen receptors and androgen receptors in a ligand-dependent manner (24), indicating the potential role of bHLH-PAS proteins, including AhR, to be able to display an E3 ligase activity with a ubiquitin family protein, in addition to its transcriptional activity.

In the nucleus, unmodified Arnt interacts and colocalizes with PML, which enhances the transactivation activity of Arnt; in contrast, SUMOylated Arnt dissociates from PML, resulting in the suppression of Arnt transcription activity in the GAL4DBD-Arnt-mediated transactivation assay (17). In contrast to AhRR, SUMOylation of Arnt is enhanced by PIAS1, and a substantial amount of Arnt is present in the nucleus in SUMOylated form (17). When AhRR is synthesized and transported into the nucleus through the NLS signal, AhRR may form a heterodimer with Arnt or SUMOylated Arnt, resulting in the enhanced SUMOylation of AhRR in the heterodimer complex. Thus, the SUMOylated AhRR and Arnt complex becomes competent for recruitment of corepressor components such as ANKRA2, HDAC4, and HDAC5. It remains to be investigated whether this series of transcription suppressor complexes are formed directly on the XRE sequence of the target genes or in the nucleoplasm prior to DNA binding. Our previous data showed that treatment of ANKRA2 small interfering RNA resulted in reduction of the AhRR-mediated repression of *Cyp1a1* mRNA expression under normal conditions (8). Because transcriptional inhibition by the AhRR·Arnt

complex is reversed by trichostatin A, an inhibitor of histone deacetylase (8), not only competitive binding to the XRE sequence, but also the HDAC activity of the AhRR/Arnt heterodimer is involved in repression by the AhRR/Arnt heterodimer. In Figs. 3 and 6, AhRR 3KR also showed some repression activity even if all SUMOylation sites are mutated, which could be explained by the residual interaction of AhRR 3KR with ANKRA2, HDAC4, and HDAC5 or competitive binding mechanisms for the XRE sequence with the AhR/Arnt heterodimer (Figs. 3*B* and 6*B*).

In this study, we have revealed a novel mechanism of transcriptional repression by the AhRR/Arnt heterodimer involving SUMO-1 modification. Further studies are required to reveal the detailed molecular mechanisms by which AhRR and Arnt are SUMOylated and subsequently recruit the corepressor components, as well as the temporal relationship between these events and the switching on/off of the target genes.

Acknowledgment—We thank Y. Nemoto for clerical work.

REFERENCES

1. Mimura, J., Ema, M., Sogawa, K., and Fujii-Kuriyama, Y. (1999) *Genes Dev.* **13,** 20–25
2. Baba, T., Mimura, J., Gradin, K., Kuroiwa, A., Watanabe, T., Matsuda, Y., Inazawa, J., Sogawa, K., and Fujii-Kuriyama, Y. (2001) *J. Biol. Chem.* **276,** 33101–33110
3. Karchner, S. I., Franks, D. G., Powell, W. H., and Hahn, M. E. (2002) *J. Biol. Chem.* **277,** 6949–6959
4. Nishihashi, H., Kanno, Y., Tomuro, K., Nakahama, T., and Inouye, Y. (2006) *Biol. Pharm. Bull.* **29,** 640–647
5. Hosoya, T., Harada, N., Mimura, J., Motohashi, H., Takahashi, S., Nakajima, O., Morita, M., Kawauchi, S., Yamamoto, M., and Fujii-Kuriyama, Y. (2008) *Biochem. Biophys. Res. Commun.* **365,** 562–567
6. Zudaire, E., Cuesta, N., Murty, V., Woodson, K., Adams, L., Gonzalez, N., Martinez, A., Narayan, G., Kirsch, I., Franklin, W., Hirsch, F., Birrer, M., and Cuttitta, F. (2008) *J. Clin. Investig.* **118,** 640–650
7. Kanno, Y., Takane, Y., Izawa, T., Nakahama, T., and Inouye, Y. (2006) *Biol. Pharm. Bull.* **29,** 1254–1257
8. Oshima, M., Mimura, J., Yamamoto, M., and Fujii-Kuriyama, Y. (2007) *Biochem. Biophys. Res. Commun.* **364,** 276–282
9. Hay, R. T. (2005) *Mol. Cell* **18,** 1–12
10. Meulmeester, E., and Melchior, F. (2008) *Nature* **452,** 709–711
11. Mizushima, S., and Nagata, S. (1990) *Nucleic Acids Res.* **18,** 5322
12. Sekine, H., Mimura, J., Yamamoto, M., and Fujii-Kuriyama, Y. (2006) *J. Biol. Chem.* **281,** 37507–37516
13. Sogawa, K., Nakano, R., Kobayashi, A., Kikuchi, Y., Ohe, N., Matsushita, N., and Fujii-Kuriyama, Y. (1995) *Proc. Natl. Acad. Sci. U. S. A.* **92,** 1936–1940
14. Gong, L., and Yeh, E. T. (2006) *J. Biol. Chem.* **281,** 15869–15877
15. Motohashi, H., Katsuoka, F., Miyoshi, C., Uchimura, Y., Saitoh, H., Francastel, C., Engel, J. D., and Yamamoto, M. (2006) *Mol. Cell. Biol.* **26,** 4652–4663
16. Johnson, E. S. (2004) *Annu. Rev. Biochem.* **73,** 355–382
17. Tojo, M., Matsuzaki, K., Minami, T., Honda, Y., Yasuda, H., Chiba, T., Saya, H., Fujii-Kuriyama, Y., and Nakao, M. (2002) *J. Biol. Chem.* **277,** 46576–46585
18. Hietakangas, V., Anckar, J., Blomster, H. A., Fujimoto, M., Palvimo, J. J., Nakai, A., and Sistonen, L. (2006) *Proc. Natl. Acad. Sci. U. S. A.* **103,** 45–50
19. Yang, X. J., and Gregoire, S. (2006) *Mol. Cell* **23,** 779–786
20. Yamashita, D., Yamaguchi, T., Shimizu, M., Nakata, N., Hirose, F., and Osumi, T. (2004) *Genes Cells* **9,** 1017–1029
21. Gregoire, S., and Yang, X. J. (2005) *Mol. Cell. Biol.* **25,** 2273–2287
22. Kang, J., Gocke, C. B., and Yu, H. (2006) *BMC Biochem.* **7,** 5
23. Shalizi, A., Gaudilliere, B., Yuan, Z., Stegmuller, J., Shirogane, T., Ge, Q., Tan, Y., Schulman, B., Harper, J. W., and Bonni, A. (2006) *Science* **311,** 1012–1017
24. Ohtake, F., Baba, A., Takada, I., Okada, M., Iwasaki, K., Miki, H., Takahashi, S., Kouzmenko, A., Nohara, K., Chiba, T., Fujii-Kuriyama, Y., and Kato, S. (2007) *Nature* **446,** 562–566

Am J Physiol Endocrinol Metab 296: E721–E730, 2009.
First published January 13, 2009; doi:10.1152/ajpendo.90829.2008.

Dual suppression of adipogenesis by cigarette smoke through activation of the aryl hydrocarbon receptor and induction of endoplasmic reticulum stress

Tsuyoshi Shimada,[1] Nobuhiko Hiramatsu,[1] Kunihiro Hayakawa,[1] Shuhei Takahashi,[1] Ayumi Kasai,[1] Yasuhiro Tagawa,[1] Mai Mukai,[1] Jian Yao,[1] Yoshiaki Fujii-Kuriyama,[2] and Masanori Kitamura[1]

[1]*Department of Molecular Signaling, Interdisciplinary Graduate School of Medicine and Engineering, University of Yamanashi, Chuo, Yamanashi; and* [2]*The Center for Tsukuba Advanced Research Alliance, University of Tsukuba, Tennodai, Tsukuba, Japan*

Submitted 9 October 2008; accepted in final form 6 January 2009

Shimada T, Hiramatsu N, Hayakawa K, Takahashi S, Kasai A, Tagawa Y, Mukai M, Yao J, Fujii-Kuriyama Y, Kitamura M. Dual suppression of adipogenesis by cigarette smoke through activation of the aryl hydrocarbon receptor and induction of endoplasmic reticulum stress. *Am J Physiol Endocrinol Metab* 296: E721–E730, 2009. First published January 13, 2009; doi:10.1152/ajpendo.90829.2008.—Cigarette smoking decreases body weight, whereas molecular mechanisms underlying this phenomenon have not been elucidated. In this report, we investigated regulation of adipogenesis by cigarette smoke and involvement of aryl hydrocarbon receptor (AhR) and endoplasmic reticulum (ER) stress. We found that cigarette smoke extract (CSE) inhibited differentiation of preadipocytes into adipocytes dose dependently. It was associated with a decrease in lipid accumulation, blunted expression of adipocyte markers (adiponectin, PPAR-γ, and C/EBPα), and sustained expression of a preadipocyte marker MCP-1. CSE markedly induced activation of AhR, and AhR agonists (2,3,7,8-tetrachlorodibenzo-*p*-dioxin, benzo[*a*]pyrene and 3-methylcholanthrene) reproduced the inhibitory effect of CSE on adipocyte differentiation. Furthermore, knockout of the AhR gene or blockade of AhR by a dominant-negative mutant attenuated the suppressive effects of CSE on adipocyte differentiation. We also found that CSE induced ER stress in preadipocytes, and ER stress inducers (thapsigargin, tunicamycin, and A23187) reproduced the suppressive effect of CSE on the differentiation of preadipocytes. Interestingly, AhR agonists did not cause ER stress, and ER stress inducers did not activate AhR. These results suggested that cigarette smoke has the potential to inhibit adipocyte differentiation via dual, independent mechanisms, i.e., through activation of the AhR pathway and induction of the unfolded protein response.

adipocyte; adiponectin; peroxisome proliferator-activated receptor-γ; CCAAT/enhancer-binding protein-α; monocyte chemoattractant protein-1

PREVIOUS INVESTIGATION suggested a link between cigarette smoking and a reduced gain of body weight. Albanes et al. (2) showed that *1*) cigarette smokers were leaner than nonsmokers, *2*) duration of smoking and body weight was inversely correlated, and *3*) these phenomena were observed in both sexes and among all ages. Although some reports suggested that smoking may decrease body weight by suppression of appetite, other cross-sectional studies showed that caloric intake was not different between smokers and nonsmokers (39). Animal experiments also showed no acute effects of smoking or nicotine administration on caloric intake (39). Currently, therefore, mechanisms underlying the suppressive effect of smoking on body weight gain are not well-understood. Because substances in cigarette smoke enter from the respiratory tracts into the systemic circulation, there is a possibility that some chemicals in smoke reach and affect the adipose tissue directly, leading to inhibition of adipogenesis and body weight gain (12). Using cultured preadipocytes, we tested this possibility and found that cigarette smoke has the potential to inhibit differentiation of preadipocytes into mature adipocytes in vitro. The aim of the present investigation is to elucidate molecular mechanisms underlying this novel observation.

In the first part of this study, we focus on a role of the aryl hydrocarbon receptor (AhR). Using gas chromatography-mass spectrometric analysis, previous investigation demonstrated that cigarette smoke contains low levels of dioxins, dioxin-like compounds, and other agonists of AhR. Those chemicals were polychlorinated dibenzo-*p*-dioxins (PCDDs), polychlorinated dibenzofurans (PCDFs), coplanar polychlorinated biphenyls (Co-PCBs), and polycyclic aromatic hydrocarbons including benzo[*a*]pyrene (B[*a*]P) (15, 33, 35). Using a cell-based bioassay to detect and quantify the level of AhR activation (25, 26), we disclosed that cigarette smoke has the high level of dioxin-like potential to activate the AhR pathway in hepatoma cells (24). Using transgenic sensor mice to monitor AhR activation in vivo, we also provided evidence that exposure of mice to cigarette smoke induced activation of AhR not only in the lung but also in other organs (23). Because AhR may be a putative, negative regulator of adipogenesis (3), AhR agonists in cigarette smoke might inhibit adipocyte differentiation.

In the second part of this investigation, we focus on a role of endoplasmic reticulum (ER) stress. The ER plays an important role in appropriate folding of synthesized proteins. Chemical, physical, and nutritional stress perturbs function of the ER, leading to accumulation of unfolded proteins in the ER (42). Such ER stress triggers several cascades of signal transduction pathways, known as the unfolded protein response (UPR), and affects cellular function. Recently, we reported that *1*) cigarette smoke induced ER stress in bronchial epithelial cells (48) and *2*) K-7174, a GATA inhibitor, suppressed adipocyte differentiation via induction of ER stress (44). ER stress and consequent UPR are known to regulate differentiation of some cell types including plasma cells, pancreatic β cells, hepatocytes, osteoblasts, and myocytes (31). Cigarette smoke could inhibit differentiation of preadipocytes via induction of ER stress.

Address for reprint requests and other correspondence: M. Kitamura, Dept. of Molecular Signaling, Interdisciplinary Graduate School of Medicine and Engineering, Univ. of Yamanashi, Shimokato 1110, Chuo, Yamanashi 409-3898, Japan (e-mail: masanori@yamanashi.ac.jp).

The costs of publication of this article were defrayed in part by the payment of page charges. The article must therefore be hereby marked "*advertisement*" in accordance with 18 U.S.C. Section 1734 solely to indicate this fact.

Based on these previous findings, we here investigate whether and how cigarette smoke suppresses adipogenesis, especially focusing on the roles of the AhR pathway and the ER stress response.

MATERIALS AND METHODS

Reagents. Insulin, 3-isobutyl-1-methylxanthine (IBMX), dexamethasone, Oil Red O, tunicamycin, thapsigargin, A23187, and 3-methylcholanthrene (3MC) were purchased from Sigma (Tokyo, Japan). 2,3,7,8-Tetrachlorodibenzo-*p*-dioxin (TCDD) and B[*a*]P were obtained from Wako Pure Chemical (Osaka, Japan). The concentrations of these agents used for studies were not toxic to 3T3-L1 cells when examined by microscopic analysis and formazan assay.

Preparation of cigarette smoke extract. To prepare cigarette smoke extract (CSE), mainstream smoke was made from 10-mg-tar cigarettes using constant vacuum flow (10.5 l/min) and collected in a glass bottle, as described previously (23, 48). The smoke from 20 cigarettes was dissolved in 500 ml PBS with vigorous shaking. This undiluted material was regarded as 100% CSE. CSE was stored at −80°C until use.

Induction of adipocyte differentiation. 3T3-L1 preadipocytes purchased from Health Science Research Resources Bank (Osaka, Japan) were maintained in DMEM-F12 (Wako Pure Chemical) supplemented with 10% FBS (basal medium). For the induction of adipocyte differentiation, cells were *1*) precultured in basal medium for 2 days, *2*) treated with differentiation medium containing 10 μg/ml insulin, 0.25 μM dexamethasone, and 500 μM IBMX (IDI medium) for 2 days, and *3*) incubated in basal medium supplemented with insulin alone for 2 days. The cells were further incubated in basal medium for an additional 2 days and subjected to analyses. To examine effects of CSE, AhR agonists, and ER stress inducers, cells were exposed to the individual agents during the initial 24-h incubation in IDI medium.

Establishment of stable transfectants. Using electroporation, 3T3-L1 cells were transfected with pEFBOS-AhR(Arg39) (47) that encodes a dominant-negative mutant of AhR (AhR-DN) under the control of the elongation factor-1α promoter (9 μg) together with pcDNA3.1 (3 μg; Invitrogen, Carlsbad, CA) that codes for neomycin phosphotransferase. Stable transfectants were selected by G418 (500 μg/ml), and 3T3-L1/AhR-DN cells were established. 3T3-L1/Neo cells were also established as a control by transfection of 3T3-L1 cells with pcDNA3.1 alone.

Primary culture of preadipocytes. Primary cultures of preadipocytes were established as described previously (7). In brief, inguinal fat pads were obtained from wild-type C57BL/6J mice and AhR-null mutant mice (34) and digested in DMEM-F12 containing 2 mg/ml collagenase-1 (Sigma) for 15 min at 37°C with gentle shaking. After gentle pipetting for a few minutes with a P-1000 micropipette, the tissues were passed through a 106-μm mesh, and the resulting cell suspension was centrifuged at 700 *g* for 10 min to separate the stromal-vascular cells from adipocytes. The pellet was washed and cultured using DMEM-F12 containing 10–20% FBS. Animals were used for the experiments according to regulations and guidelines at

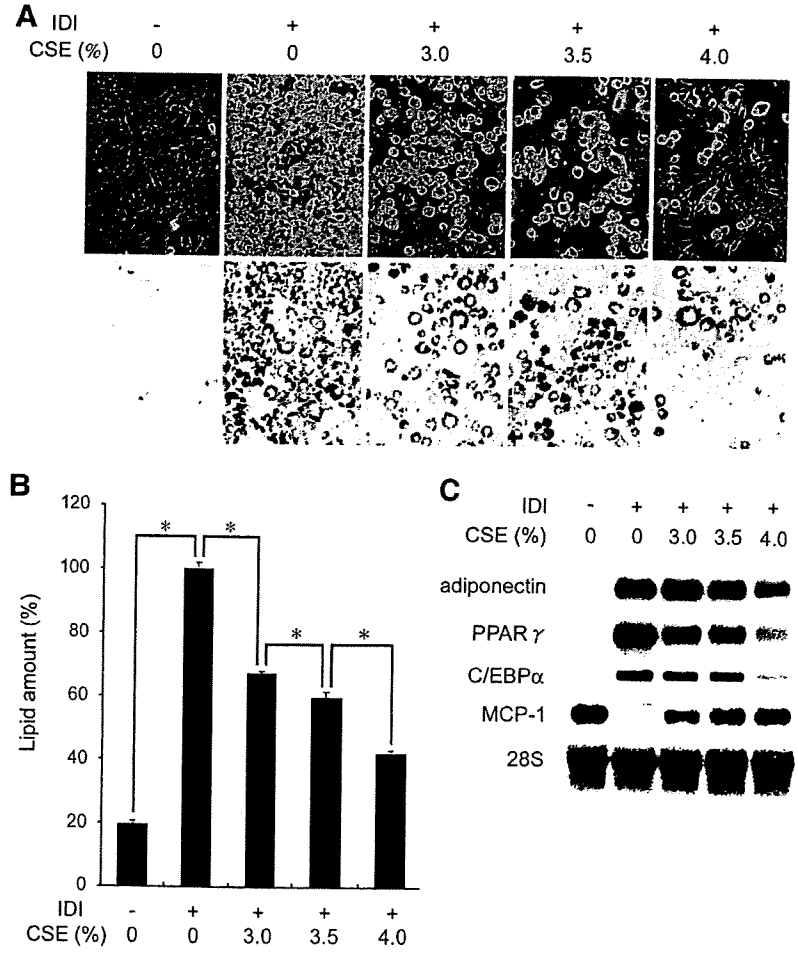

Fig. 1. Blockade of adipocyte differentiation by cigarette smoke extract (CSE). 3T3-L1 preadipocytes were pretreated with serial concentrations of CSE for 6 h and treated with insulin, dexamethasone, and IBMX (IDI) in the presence of CSE. After 24 h, the cells were further cultured in the absence of CSE for an additional 5 days and subjected to microscopic analyses (*top* row, phase-contrast microscopy; *bottom* row, Oil Red O staining; *A*), quantitative analysis of lipid content (*B*), and Northern blot analysis of adiponectin, peroxisome proliferator-activated receptor-γ (PPAR-γ), CCAAT/enhancer-binding protein-α (C/EBPα), and monocyte chemoattractant protein-1 (MCP-1) (*C*). The level of 28S ribosomal RNA was used as a loading control. *B*: assays were performed in quadruplicate. Data are expressed as means ± SE, and *statistically significant differences ($P < 0.05$).

University of Yamanashi. The experiments were approved by the Yamanashi University Animal Experiment Committee.

Oil Red O staining. To quantify lipid accumulation, cells were fixed with 10% formalin in PBS for 10 min, rinsed with 60% isopropanol, and stained by Oil Red O in 60% isopropanol for 20 min. After the staining, cells were rinsed several times with 60% isopropanol and subjected to microscopic analysis. To evaluate the amount of lipid quantitatively, cells were added with isopropanol containing 4% Nonidet P-40 and lysed by agitation for 5 min. Absorbance (520-nm wave length) was measured by a spectrophotometer.

Northern blot analysis. Northern blot analysis was performed as described before (30). cDNAs for adiponectin (49), peroxisome proliferator-activated receptor-γ (PPAR-γ; purchased from Addgene, Cambridge, MA) (20), CCAAT/enhancer binding protein (C/EBP)-α (6), monocyte chemoattractant protein-1 (MCP-1) (41), 78-kDa glucose-regulated protein (GRP78) (28), C/EBP-homologous protein (CHOP) (50), AhR (47), and cytochrome *P*-4501B1 (CYP1B1) (45) were used for preparation of radiolabeled probes. The levels of 28S ribosomal RNA and glyceraldehyde-3-phosphate dehydrogenase mRNA were used as loading controls. Assays were repeated two to three times, and representative results were shown.

Dioxin-responsive element-based sensing via secreted alkaline phosphatase assay. Dioxin-responsive element-based sensing via secreted alkaline phosphatase (DRESSA) bioassay was performed using HeXS34 cells to evaluate activity of AhR (25–27). Activity of secreted alkaline phosphatase (SEAP) in culture media was evaluated by a chemiluminescent method using Great EscAPe SEAP Detection Kit (BD Biosciences, Palo Alto, CA), as described before (26).

ER stress-responsive alkaline phosphatase assay. Induction of ER stress was evaluated by ER stress-responsive alkaline phosphatase (ES-TRAP) assay (21). 3T3-L1 cells were transiently transfected with pSEAP2-Control (BD Biosciences) by using GeneJuice Transfection Reagent (Novagen, Madison, WI) and treated with test reagents. Activity of ES-TRAP in culture medium was evaluated using Great EscAPe SEAP Detection Kit.

Formazan assay. The number of viable cells was assessed by formazan assay using Cell Counting Kit-8 (Dojindo Laboratory, Kumamoto, Japan) (21).

Statistical analysis. Data were expressed as means ± SE. Statistical analysis was performed using the nonparametric Mann-Whitney *U*-test to compare data in different groups. A P value of <0.05 was considered to be a statistically significant difference.

RESULTS

Blockade of adipocyte differentiation by CSE. To examine whether cigarette smoke has the potential to affect differentiation of preadipocytes into adipocytes, 3T3-L1 preadipocytes were pretreated with serial concentrations of CSE for 6 h and treated with IDI medium (differentiation medium) in the presence of CSE. After 24 h, the cells were further incubated in IDI medium without CSE for an additional 24 h. After the incubation, the cells were cultured in basal medium supplemented with insulin for 2 days, further incubated in basal medium for an additional 2 days, and subjected to microscopic analyses. As shown Fig. 1*A*, in the absence of CSE, IDI medium induced differentiation of preadipocytes into adipocytes with substantial lipid accumulation. Treatment with CSE inhibited this process in a concentration-dependent manner. Oil Red O staining revealed that accumulation of lipid was significantly reduced to 67.0 ± 1.1% by 3% CSE and to 42.1 ± 0.9% by 4% CSE vs. 100% in CSE-untreated cells (means ± SE, $P < 0.05$; Fig. 1*B*).

It is known that, during differentiation of 3T3-L1 preadipocytes, expression of adiponectin, PPAR-γ, and C/EBPα increases dramatically (9, 11, 22), whereas basal expression of MCP-1 is suppressed (16). To confirm the inhibitory effect of cigarette smoke on adipocyte differentiation, 3T3-L1 cells were treated with IDI containing CSE for 24 h, further incubated for an additional 5 days as described above, and subjected to Northern blot analysis. As shown in Fig. 1*C*, expression of adipocyte markers adiponectin, PPAR-γ, and C/EBPα was induced during adipocyte differentiation, whereas this induction was attenuated by CSE in a dose-dependent manner. In contrast, expression of the preadipocyte marker MCP-1 was suppressed during adipocyte differentiation, whereas this inhibitory effect was abolished by CSE. These results confirmed that CSE inhibited adipocyte differentiation.

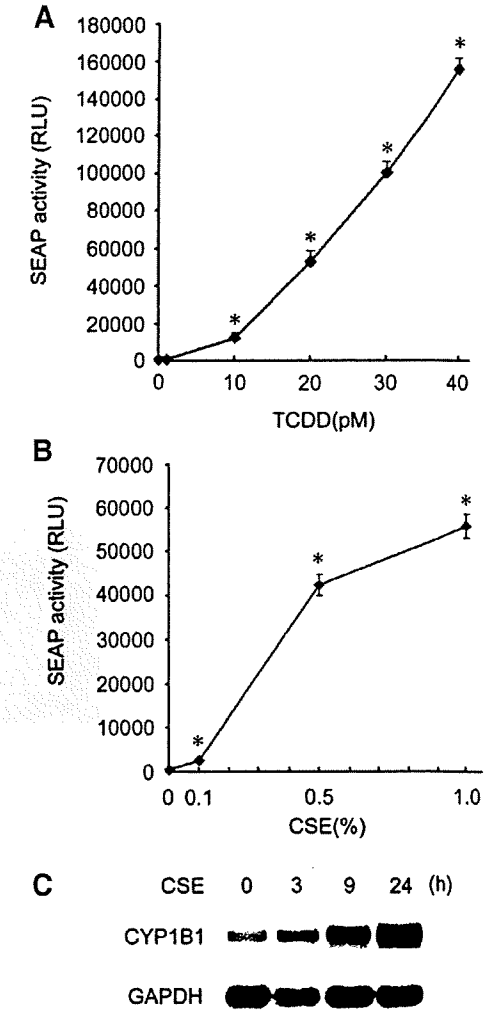

Fig. 2. Activation of the aryl hydrocarbon receptor (AhR) by CSE. *A* and *B*: reporter cells that produce secreted alkaline phosphatase (SEAP) following activation of AhR were exposed to serial concentrations of 2,3,7,8-tetrachlorodibenzo-*p*-dioxin (TCDD; *A*) or CSE (*B*) for 24 h, and activity of SEAP in culture media was evaluated by chemiluminescent assay. Assays were performed in quadruplicate. Data are expressed as means ± SE. *Statistically significant differences ($P < 0.05$). RLU, relative light unit. *C*: 3T3-L1 preadipocytes were treated with 4% CSE for indicated time periods and subjected to Northern blot analysis of cytochrome *P*-4501B1 (CYP1B1). The level GAPDH mRNA is shown at the *bottom* as a loading control.

Inhibition of adipocyte differentiation by CSE through activation of AhR. A previous report indicated that AhR may be a putative, negative regulator of adipogenesis (3). Cigarette smoke contains dioxins, dioxin-like compounds, and other agonists of AhR, which might inhibit adipocyte differentiation via activation of AhR. To test this possibility, we first examined the potential of cigarette smoke to activate AhR using the DRESSA assay (25, 26). Reporter cells were exposed to serial concentrations of TCDD or CSE, and activity of the reporter enzyme SEAP was evaluated by chemiluminescent assay. As expected, TCDD caused activation of AhR dose dependently (Fig. 2*A*). Similarly, CSE induced activation of AhR in a dose-dependent manner (Fig. 2*B*). This result was further confirmed using an endogenous indicator for AhR activation in adipocytes, CYP1B1 (3). Consistent with the result from the DRESSA assay, Northern blot analysis revealed that CSE substantially induced expression of CYP1B1 in preadipocytes (Fig. 2*C*), confirming the activation of AhR.

We next examined effects of AhR agonists on the differentiation of preadipocytes. 3T3-L1 cells were treated with IDI in the presence of TCDD, B[*a*]P, or 3MC for 24 h, and morphologic examination was performed after 5 days. As shown in Fig. 3*A*, adipocyte differentiation was inhibited markedly by B[*a*]P and 3MC and moderately by TCDD. It was associated with marked suppression of lipid accumulation by B[*a*]P and 3MC and moderate inhibition by TCDD (Fig. 3*B*). Consistent with this result, Northern blot analysis revealed that IDI-induced expression of adipocyte markers (adiponectin, PPAR-γ, and C/EBPα) was suppressed by B[*a*]P and that suppression of the preadipocyte marker MCP-1 by IDI was abrogated by this AhR agonist (Fig. 3*C*).

To confirm the role of AhR in the suppression of adipocyte differentiation, we established 3T3-L1 cells overexpressing a dominant-negative mutant of AhR, AhR-DN (Fig. 4*A*), and the effect of CSE was retested. As shown in Fig. 4*B* (*top* rows), CSE and TCDD inhibited adipocyte differentiation in mock-transfected 3T3-L1/Neo cells. However, this inhibitory effect was attenuated in 3T3-L1/AhR-DN cells (Fig. 4*B*, *bottom* rows). Oil Red O staining revealed that the suppression of lipid accumulation by CSE and TCDD was partially but significantly reversed by dominant-negative inhibition of AhR (Fig. 4*C*). To further confirm our conclusion, we also established preadipocytes from adipose tissues in wild-type mice and AhR-null mutant mice. Morphologically, both preadipocytes exhibited undistinguishable features (Fig. 4*D*, *lane 1*). After stimulation with IDI, both cell types similarly differentiated into adipocytes (Fig. 4*D*, *lane 2*). However, consistent with the result from 3T3-L1/AhR-DN cells, the AhR-null preadipocytes exhibited insensitiveness to CSE- and TCDD-induced suppression of adipocyte differentiation (Fig. 4*D*, *lanes 3* and *4*). Quantitative analysis revealed that the suppression of adipogenesis by CSE and TCDD was markedly attenuated in AhR-null cells (Fig. 4*E*), confirming the crucial role of AhR in the anti-adipogenic effect of cigarette smoke.

Inhibition of adipocyte differentiation via ER stress triggered by CSE. Recently, we reported that K-7174 suppressed adipocyte differentiation and that it was associated with induction of ER stress (44). We also showed that, in bronchial

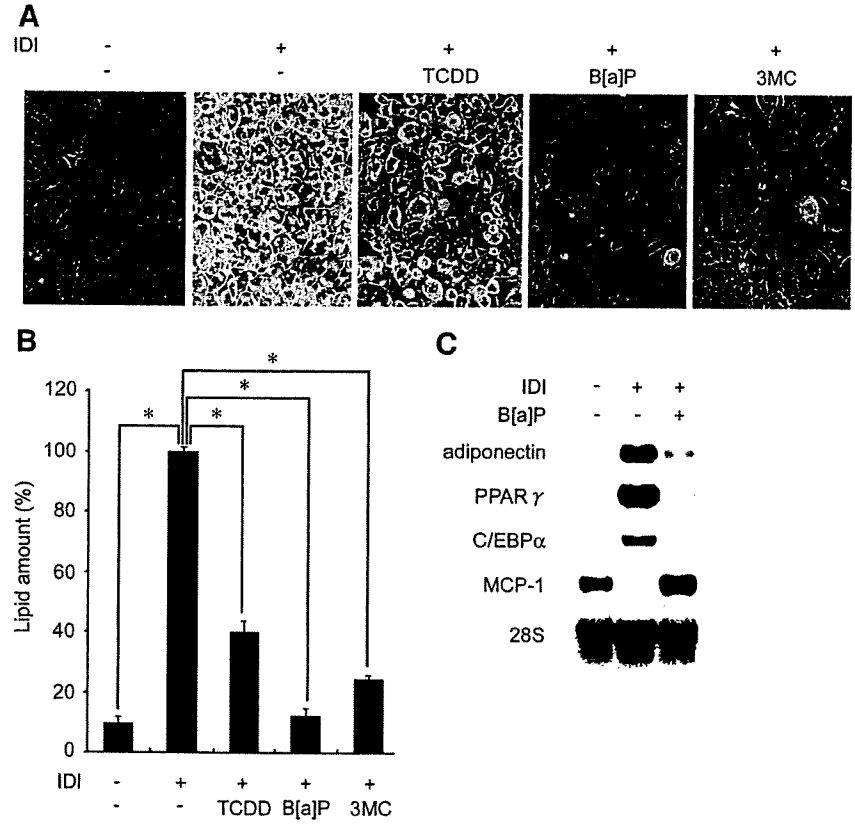

Fig. 3. Inhibition of adipocyte differentiation by AhR agonists. 3T3-L1 preadipocytes were treated with IDI in the presence of AhR agonists including TCDD (10 nM), benzo[*a*]pyrene (B[*a*]P; 1 μM), and 3-methylcholanthrene (3MC; 5 μM) and subjected to phase-contrast microscopy (*A*), quantitative analysis of lipid content (*B*), and Northern blot analysis of adiponectin, PPAR-γ, C/EBPα, and MCP-1 (*C*). *B*: assays were performed in quadruplicate. Data are expressed as means ± SE. *Statistically significant differences ($P < 0.05$).

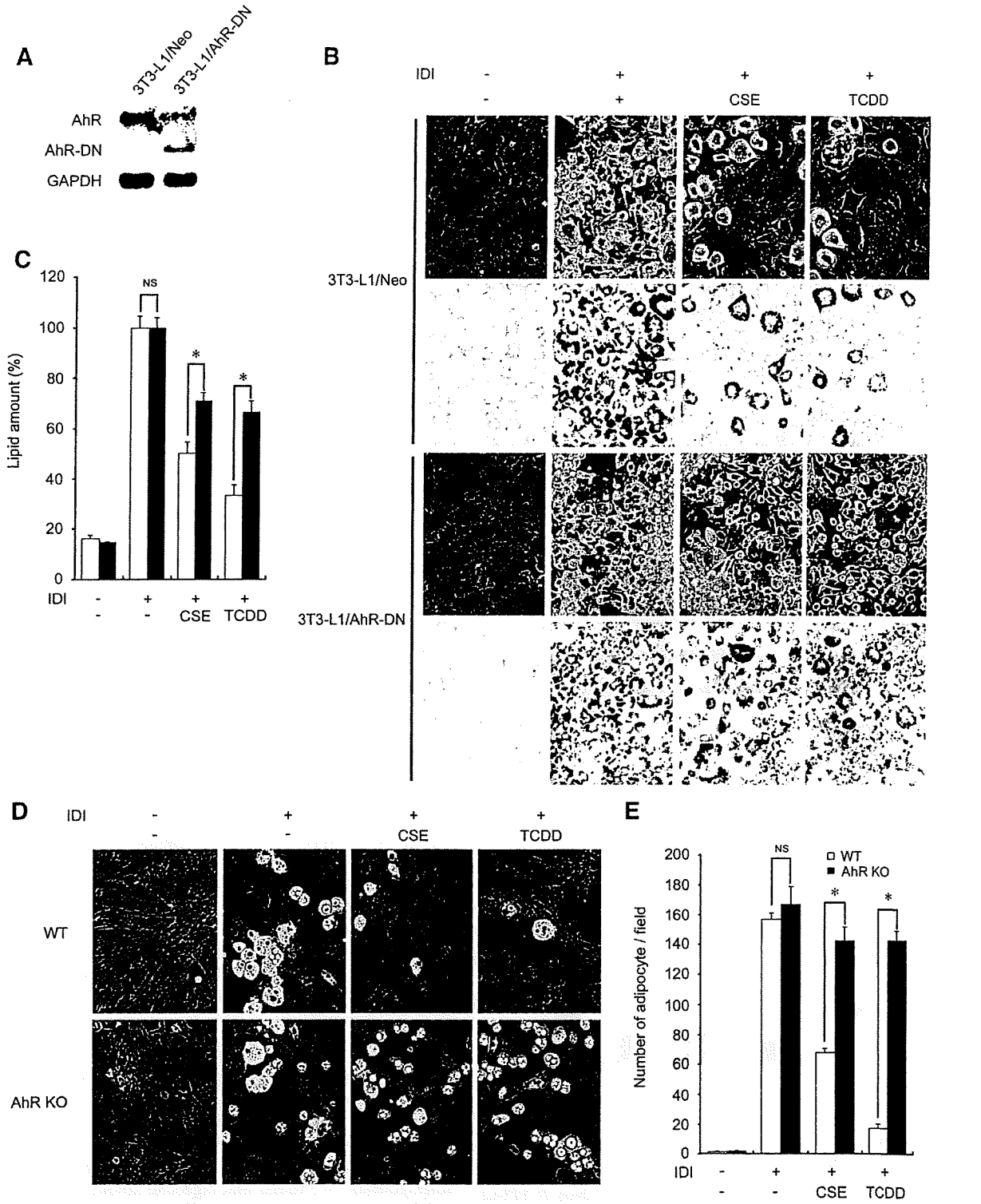

Fig. 4. Attenuation of anti-adipogenic effects of CSE in the absence of AhR. *A–C*: 3T3-L1 cells were stably transfected with a dominant-negative mutant of AhR (AhR-DN), and 3T3-L1/AhR-DN cells were established. Expression of endogenous AhR and exogenous AhR-DN in 3T3-L1/AhR-DN cells and mock-transfected 3T3-L1/Neo cells was examined by Northern blot analysis (*A*). The cells were then treated with IDI in the presence of CSE (4%) or TCDD (10 nM) and subjected to microscopic analyses (*B*) and quantitative analysis of lipid content (*C*). *D* and *E*: preadipocytes were established from adipose tissues in wild-type mice (WT) and AhR-null mutant mice (AhR KO). The cells were then treated with IDI in the presence of CSE or TCDD and subjected to phase-contrast microscopy (*D*) and quantitative analysis of the number of mature adipocytes (*E*). *C* and *E*: assays were performed in quadruplicate. Data are expressed as means ± SE. *Statistically significant differences ($P < 0.05$). NS, not statistically significant.